Ecological Monographs, 76(2), 2006, pp. 175–194

MULTITROPHIC BIOPHYSICAL BUDGETS: THERMAL ECOLOGY OF AN INTIMATE HERBIVORE INSECT–PLANT INTERACTION

Sylvain Pincebourde[1] and Jérôme Casas

Institut de Recherche sur la Biologie de l'Insecte (IRBI, CNRS UMR 6035), Université François Rabelais, Faculté des Sciences et Techniques, 37200 Tours, France

Abstract. Physiology of ectothermic organisms depends on microclimate temperature. In some insect–plant relationships, the herbivore physically manipulates its proximate environment (i.e., plant tissues). However, little is known about the effects of this manipulation on the insect microclimate. We studied the thermal environment of the leaf-mining insect *Phyllonorycter blancardella* (Lepidoptera: Gracillariidae). This herbivore modifies both morphology and physiology of attacked apple leaf tissues to construct a mine inside which the entire larval development occurs. Spectral measurements showed that absorbance of mined leaf tissues differed from that of intact leaf tissues. Gas exchange measurements in mined leaf tissues demonstrated that responses of stomata to changes in climatic parameters were modified compared to intact leaf tissues. We built an energy budget model to predict the temperature within a mine given climatic variables, and measured parameters related to radiative absorption properties and to the ecophysiology of stomata. Model predictions were verified using experimental measurements made under a large range of climatic conditions. Radiation level was the most influential variable on both mine and leaf temperatures, and a mine was always warmer than a leaf. Mine temperature was predicted to be up to 10°C above ambient air and 5°C warmer than intact leaf tissues at high radiation levels. The decoupling between mine temperature and leaf temperature was significant. The model was manipulated to quantify the separate effects of altered absorbance and modified stomatal behavior. Both effects contributed almost equally to the temperature excess. A mine gained more radiative heat than a leaf and the observed stomatal closure limited latent heat losses. We suggest that this warm microclimate allows larvae to develop faster, leading to a reduced risk of attack by parasitoids. The model, which is the most complete one to date for any herbivorous insect, shows that the second trophic level manages and partially controls the first one, even to the point of one trophic partner co-opting the physiology of the other. These reciprocal influences imply that heat budgets cannot be simply built for each trophic level independently.

Key words: *body temperature; energy budget; heat transfer; leaf miner; leaf temperature; microclimate;* Phyllonorycter blancardella; *radiation absorption; stomatal conductance; thermal environment.*

Introduction

Temperature is a strong selection pressure for ectothermic organisms that respond through two main mechanisms. Some species behaviorally select a thermal environment naturally present in their habitat that permits some optimal or at least survivable range of body temperatures. In this case, habitat selection has strong consequences on the organism physiology and species are expected to develop sensory and behavioral mechanisms allowing detection and discrimination of a suitable thermal environment (Huey 1991). The use of thermal cues to detect a favorable thermal environment has been found, for example, in reptiles (e.g., Pringle et al. 2003) and arthropods (e.g., Goldsbrough et al. 2004). Other species have evolved physiological and behavioral processes that allow them to directly modify their microclimate by manipulating their physical microhabitat (Danks 2002). Selection pressures partly act on strategies used by organisms to modify their proximate environment, which in turn provides them with an altered thermal environment. A beautiful example is given by the social tent-building caterpillars *Eriogaster lanestris*. The tent wall, built by the larvae, shields the tent from most incoming radiation and reduces heat exchange with ambient air. This allows caterpillars to stabilize their body temperature over a wide range of ambient temperatures by adjusting the level of collective metabolic heat production (Ruf and Fiedler 2000, 2002).

Body temperature has a pervading influence on most biological functions in insect species, including metabolic rate (e.g., van Loon et al. 2005), feeding rate (e.g., Kingsolver 2000), development time (e.g., Gilbert and Raworth 1996, Rombough 2003), mate location (e.g., Van Dyck and Matthysen 1998), and general physiological performance (e.g., Huey and Kingsolver 1989). Predicting body temperature is a difficult task because it could be influenced by both abiotic variables of the

Manuscript received 21 July 2005; revised 28 October 2005; accepted 3 November 2005. Corresponding Editor: T. D. Williams.

[1] E-mail: sylvain.pincebourde@univ-tours.fr.

microclimate (e.g., microclimate temperature, incoming radiation, and relative humidity) and biotic elements positioned close to the organism (e.g., conspecifics, predators), as well as by characteristics of the organism itself. Thus, feedback loops can be expected between abiotic and biotic factors (Helmuth 1998, 2002). Modeling heat budgets has been proven to be a powerful approach to elucidate the biophysical mechanisms determining the body temperature of many organisms (Gates 1980). This biophysical approach was applied on plant leaves (Campbell and Norman 1998, Nobel 1999), cacti (Nobel 1988), several insect species (e.g., Kingsolver and Moffat 1982, Casey 1992, Lactin and Johnson 1998), mussels (Helmuth 1998), and reptiles (e.g., Spotila et al. 1972, Grant and Porter 1992, O'Connor and Spotila 1992, O'Connor 1999). These models are highly sophisticated because they predict not only body temperature but also the relative influence of the surrounding microclimate on the organism. Thus, their flexible feature allows these models to include behavioral or physiological components of the organism (e.g., Casey 1992). However, these energy budgets usually deal with the influence of abiotic components on the thermal budget of the organism and few studies have incorporated the impact of biotic factors on an organism's temperature. Helmuth (1998) showed that the body temperature of a solitary mussel is warmer than the temperature of individuals in a mussel bed under extreme climatic conditions. Patiño et al. (1994) demonstrated that *Ficus* fruit physiology is regulated such that fruit temperature is below the upper lethal temperature of its mutualistic pollinator wasp. A few other studies tackle the thermal interaction between plants and their pollinators, but without reference to any mechanistic heat budget (e.g., Herrera 1995, Orueta 2002, Seymour et al. 2003). Furthermore, no study attempted so far has established a comprehensive heat budget of multitrophic relationships in which the budgets of both partners have been detailed. Here we use a mechanistic heat budget to explore the thermal ecology of an insect–plant relationship.

Insects living inside or at the leaf surface experience a thermal environment that is regulated by the plant. The plant thermal regulation system determines directly leaf temperature (Campbell and Norman 1998) and involves a tight control of the stomata opening level (Ziegler 1987). This mechanism allows leaf temperature to be colder or warmer by several degrees than ambient air (e.g., Jones 1999). However, some insects, such as galling insects, leaf miners, leaf rollers, and leaf tiers, do manipulate leaves and other plant parts. These insects might modify the temperature regulation system of the leaf in order to achieve an altered microclimate. For example, galls can be warmer by several degrees than ambient during sunny days. Temperature within galls remains, however, highly temporally variable (Layne 1993). Turner (2000) suggests that some galling insects live in a warm environment due to the design of their gall, which stands out of the leaf boundary layer. However, that approach remains to be experimentally confirmed (Turner 2000). Overall, very little is known about the way endophagous insects manipulate their host plant and the extent to which this may alter their microclimatic environment.

Leaf miners are sessile organisms allowing a study of the tight coupling between the insect and host plant physiology in great detail. The leaf miner *Phyllonorycter blancardella* F. (Lepidoptera: Gracillariidae) was found to induce stomatal closure in the attacked leaf parts as a result of both plant tissue reactions to the larval feeding pattern and the CO_2 released by larvae within the mine (S. Pincebourde, E. Frak, J. L. Regnard, H. Sinoquet, and J. Casas, *unpublished manuscript*). Stomatal closure considerably limits water vapor loss out of a mine and probably leads to retention of latent heat linked to evaporation. This could affect the thermal budget of a mine and thereby the temperature within it. Moreover, the leaf areas fed by leaf miners transmit most incident radiation within the mine, whereas intact tissues in the mine epidermis transmit radiation only weakly (Pincebourde and Casas 2006). Body temperature could therefore be determined not only by microhabitat temperature but also by radiation level and by the use of microhabitat by larvae (i.e., whether larvae position themselves below fed or unfed mined leaf tissues).

We investigated the thermal environment of the leaf miner *P. blancardella* in great detail. We built a biophysical model to predict the temperature within a mine from climatic, ecophysiological, and physical parameters. This model is based on the energy budget of a leaf and incorporates the measured modifications that a leaf miner causes on plant tissues. These are related to the induced changes in both optical properties of the leaf surface and stomatal behavior. Model temperature predictions were verified against experimental measurements made under controlled conditions. Model explorations allowed us to quantify the effects of these different modifications on the microclimate temperature larvae undergo and to quantify the extent of the temperature decoupling between host leaves and insect microhabitat. Body temperature was then determined using predicted mine temperatures and an empirical relationship between body-to-mine temperature deviation and radiation level.

Methods

Insects and plants

The spotted tentiform leaf miner *P. blancardella* develops on apple leaves, and larvae grow within the leaf lamina, inside a sealed sack called a "mine" (see Plate 1). Stomata in mined leaf tissues are the only bridges between the mine and the ambient atmosphere. Larval development is divided into five instars (Pottinger and LeRoux 1971). The first three instars are characterized by a sap-feeding behavior that defines the

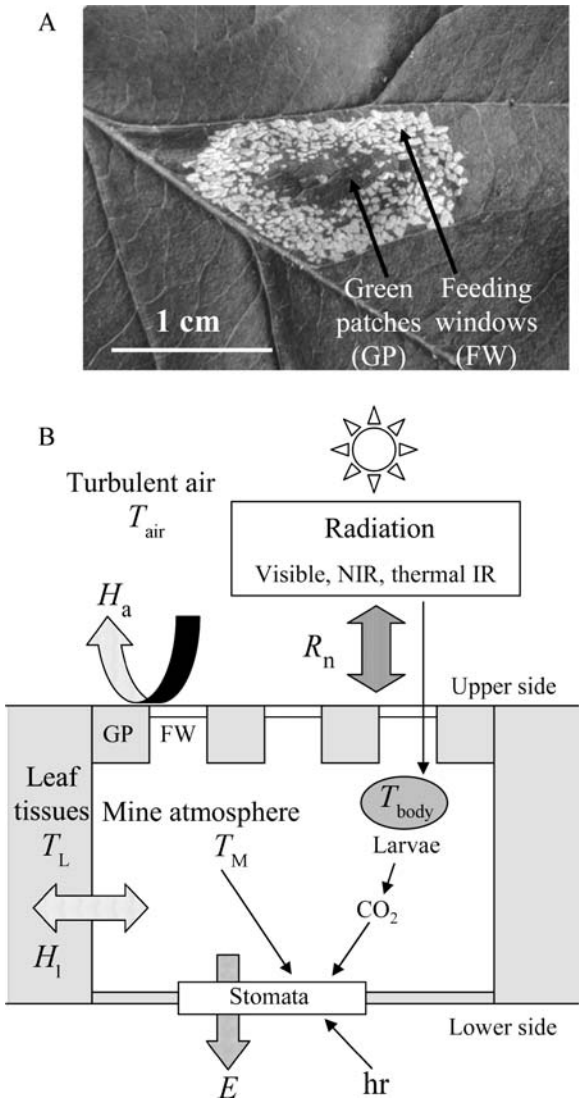

FIG. 1. Mine structure. (A) The upper surface of a mine. The feeding activity of a larva results in the formation of feeding windows (FW). Green patches (GP) correspond to intact chlorophyll-containing leaf tissues remaining in the mine. Mines of last-instar larvae are oblong shaped. (B) Schematic cross section of a mine and determinants of heat transfer. The surface of the mine is assumed to be flat. Body temperature of a larva (T_{body}) is affected by temperature within the mine (T_M) and by the amount of radiation transmitted through the feeding windows. Mine temperature is determined by (1) the net radiation budget (R_n), (2) sensible heat exchanged between the mine and ambient air (H_a), which is at temperature T_{air} (forced convection processes), (3) sensible heat exchanged between the mine and adjacent leaf tissues (H_l), which are at temperature T_L (free convection processes), and (4) latent heat lost by the mine (E) during the transpiration process through stomata. E depends on the opening level of stomata, which is affected by mine temperature, radiation level (visible), relative humidity in the air ("hr"), and the CO_2 released by the larva within the mine. A mine always contains only one larva.

outline of the mine by separating leaf tissues into upper and lower sides. Larvae are tissue feeders during the fourth and fifth instars. This feeding behavior results in the formation of translucent patches called feeding windows (Djemai et al. 2000), which remain after chlorophyll-containing tissues have been consumed (Fig. 1A). The mine of a last-instar larva usually has a surface of ~1 cm^2 and offers a relatively large space for a larva, as the upper mine integument bulges; larval volume is ~2.8 mm^3 and the total mine volume is ~95.0 mm^3 (S. Pincebourde, *unpublished data*). The lower mined leaf tissues remain flat.

Six-month-old apple seedlings (*Malus communis*) were reared in a greenhouse at mean air temperature of 19.9°C, mean relative humidity of 59.5%, and maximal irradiance 1500 $\mu mol \cdot m^{-2} \cdot s^{-1}$. Seedlings were planted in earthenware pots (11.5 cm in diameter) and watered every two days with a nutritive solution. The solution was composed (volume fraction) of 6% nitrogen, 6% P_2O_5, and 6% K_2O, completed with distilled water and mixed together. The emergence date, corresponding to full expansion of each leaf, was recorded to control for leaf age.

The leaf temperature model

The temperature of a leaf is determined by an energy balance model of a leaf (Campbell and Norman 1998, Nobel 1999), which is

$$R_n + H + E = 0. \quad (1)$$

Here, R_n represents the net radiation heat flux, H corresponds to the sensible heat flux (heat transferred by conduction and convection due to a temperature difference), and E is the latent heat flux (heat lost through water evaporation). All processes are expressed in flux rate density (W/m^2) and values are positive or negative depending on the direction of the heat transfer (heat gained or lost by the leaf, respectively). Very little energy is stored or metabolized in a leaf, so that both energy storage and heat absorption during photosynthesis can be neglected (Campbell and Norman 1998, Nobel 1999). We followed the procedures of Campbell and Norman (1998) to detail the different balances, which are averaged between upper and lower surfaces.

The net radiation budget of a leaf.—Leaves absorb radiation in the visible (or PAR, photosynthetically active radiation, from 400 nm to 700 nm), near infrared (from 800 nm to 2500 nm), and thermal infrared ranges (above 2500 nm; Campbell and Norman 1998). Leaves also emit radiation in the thermal infrared range. The net radiation budget is

$$R_n = a_L^{VIS} I^{VIS} + a_L^{NIR} I^{NIR} + a_L^{TIR} I^{TIR} - \varepsilon_L \sigma T_L^4. \quad (2)$$

The net radiation budget depends on leaf absorbance a_L^{VIS}, a_L^{NIR}, and a_L^{TIR} in the visible, near infrared, and thermal infrared ranges, respectively, and on leaf emissivity in the thermal infrared range, ε_L. These parameters determine directly the portion of the total incident radiation (direct and diffuse) that a leaf absorbs

in the visible (I^{VIS}), near infrared (I^{NIR}), and thermal infrared (I^{TIR}) regions, respectively (all in W/m^2). The emission of thermal infrared radiation by a leaf depends on the Stephan-Boltzman constant ($\sigma = 5.67 \times 10^{-8}$ W·m^{-2}·K^{-4}) and on leaf temperature T_L (K), assuming a leaf as a black body (Campbell and Norman 1998). According to the Kirchhoff's law, absorbance in the thermal infrared range equals the emissivity. This value is around 0.97 W/m^2 for leaves (i.e., $a_L^{TIR} = \varepsilon_L = 0.97$, Campbell and Norman 1998).

The sensible heat budget of a leaf.—The sensible heat flux leaving a leaf is determined by

$$H = c_p g_L^{ha}(T_L - T_{air}) \quad (3)$$

where c_p is the specific heat of the air (29.3 J·mol^{-1}·°C^{-1}), g_L^{ha} is the leaf boundary layer conductance for heat (mol·m^{-2}·s^{-1}), and T_{air} is air temperature (K). During forced convection processes, the leaf boundary layer conductance for heat is calculated from

$$g_L^{ha} = 1.4 \times 0.135\sqrt{\frac{u}{d_L}}. \quad (4)$$

The boundary layer conductance for heat depends on wind velocity, u (m/s), and on leaf characteristic dimension, d_L, (m). The factor 0.135 is obtained from values of air viscosity, air density, and air diffusivity (Campbell and Norman 1998). The characteristic dimension of a leaf is estimated from

$$d_L = 0.72\, l_L \quad (5)$$

where l_L is the maximal width of the leaf (m).

The latent heat budget of a leaf.—A leaf loses water vapor through its lower and upper tissues (stomata and epidermis, respectively). The latent heat lost during this evaporation process is determined by

$$E = \lambda g_L^{v}\left[\frac{e_s(T_L) - e_a}{p_a}\right]. \quad (6)$$

Here, λ is the latent heat of vaporization for water ($\lambda =$ 44 kJ/mol at 25°C), g_L^{v} is the leaf conductance for water vapor transfer (mol·m^{-2}·s^{-1}), $e_s(T_L)$ is the saturated water vapor pressure (Pa) at leaf temperature T_L (°C), e_a is the water vapor pressure in the air (Pa), and p_a is the atmospheric pressure ($p_a = 101.3 \times 10^3$ Pa). The term $e_s(T_L) - e_a$ corresponds to the leaf water vapor pressure deficit (D_L). Eq. 6 is based on the assumption that the internal atmosphere of a leaf is saturated for water vapor. This assumption is reasonable since relative humidity within the leaf atmosphere is higher than 95% (Nobel 1999). The Tetens empirical equation is convenient to calculate the saturation water vapor pressure from leaf temperature (°C):

$$e_s(T_L) = 0.611 \exp\left(\frac{17.502T_L}{T_L + 240.97}\right). \quad (7)$$

The water vapor pressure in the air, e_a, could be determined from air temperature and relative humidity, hr, which are parameters easier to measure than e_a, from

$$e_a = \text{hr} \times e_s(T_{air}). \quad (8)$$

Air is said to be saturated when hr = 1. The saturation water vapor pressure in the air is determined using Eq. 7. The leaf conductance for water vapor is computed by combining the boundary layer conductance (g_L^{va}) and the tissue conductance (stomatal conductance, g_L^{vs}, and epidermis conductance, g_L^{ve}) for water vapor. The leaf conductance for a hypostomatous leaf (i.e., having stomata only on the lower side, is

$$g_L^{v} = \frac{0.5}{\frac{1}{g_L^{va}} + \frac{1}{g_L^{vs}}} + \frac{0.5}{\frac{1}{g_L^{va}} + \frac{1}{g_L^{ve}}}. \quad (9)$$

The boundary layer conductance for water vapor is

$$g_L^{va} = 1.4 \times 0.147\sqrt{\frac{u}{d_L}}. \quad (10)$$

The factor 0.147 results from the use of water vapor viscosity, density, and diffusivity. The stomatal conductance is determined by environmental variables. We used the model of Jarvis (1976) according to which the effect of each variable is independent from the other (nonsynergetic interactions). Stomatal conductance was therefore calculated by

$$g_L^{vs} = g_L^{smax} f_L^1(Q) f_L^2(D_L) f_L^3(T_L) \quad (11)$$

where g_L^{smax} is the maximal stomatal conductance (mol·m^{-2}·s^{-1}), attained under specific levels of leaf irradiance (Q: μmol PAR·m^{-2}·s^{-1}), leaf water vapor pressure deficit (D_L: Pa) and leaf temperature (T_L: °C), and f_L^1, f_L^2, and f_L^3 are the functions describing the variations of the stomatal conductance relative to the maximal value following a change in leaf irradiance level, leaf water vapor pressure deficit, and leaf temperature, respectively.

The leaf temperature calculation.—Returning to Eq. 1 and replacing each term by its full expression, we solved the equation for leaf temperature using iterative procedures for nonlinear equations. The solution cannot be expressed explicitly because (1) leaf temperature is expressed at the fourth power in the thermal infrared emittance term (Eq. 2), (2) leaf temperature is expressed within an exponential in the term for saturation water vapor pressure (Eqs. 6, 7), and (3) leaf temperature is included within the complex expression of the stomatal conductance term (Eq. 11).

The mine temperature model

The model that we built computes the energy balance of a mine using the same concepts and procedures as before. The sensible heat being exchanged between a mine and adjacent leaf tissues was furthermore integrated into the model (Fig. 1B). The energy budget of a mine is then

$$R_n + H_a + R_S H_l + E = 0. \quad (12)$$

R_n is the net radiation heat flux, H_a is the sensible heat flux exchanged between a mine and ambient air, H_l is

the sensible heat flux exchanged between a mine and adjacent leaf tissues, and E is the latent heat flux (Fig. 1B). The balances R_n, H_a, and E are expressed in watts per unit of mine area (W/m^2), whereas the balance H_l is expressed in watts per unit of mine–leaf contact surface (W/m^2). We employed the term R_S to convert H_l in watts per unit of mine area. This term was calculated following

$$R_S = \frac{P_M}{S_M} \tag{13}$$

where P_M is the area of the mine–leaf interface (m^2) and S_M is the mine area (m^2).

The net radiation budget of a mine.—As for a leaf, a mine receives radiation from the visible, near infrared, and thermal infrared ranges. The net radiation budget of a mine is

$$R_n = a_M^{VIS} I^{VIS} + a_M^{NIR} I^{NIR} + a_M^{TIR} I^{TIR} - \varepsilon_M \sigma T_M^4 \tag{14}$$

where a_M^{VIS}, a_M^{NIR} and a_M^{TIR} are mine absorbance in the visible, near infrared, and thermal infrared ranges, respectively. The term of emitted thermal radiation depends on mine temperature, T_M (K) and on mine emissivity, ε_M. Since a mine is made from plant tissues we assume that $a_M^{TIR} = \varepsilon_M = 0.97$.

The sensible heat budget of a mine.—A mine is assumed to be a flat surface. Implications of this assumption are discussed later (see *Discussion: Assumptions and validity of the models*). The sensible heat flux exchanged between a mine and ambient air can be written as

$$H_a = c_p\, g_M^{ha} (T_M - T_{air}) \tag{15}$$

where g_M^{ha} is the mine boundary layer conductance for heat ($mol \cdot m^{-2} \cdot s^{-1}$). A mine (area of 1 cm^2) is considered as being a part of the leaf structure and the boundary layer is considered to be identical to the one of the whole leaf (i.e., $g_M^{ha} = g_L^{ha}$). It is therefore calculated from Eq. 4 under forced convection process. The sensible heat flux exchanged between a mine and adjacent leaf tissues is computed from

$$H_l = c_p g_{ML}^{hl} (T_M - T_L). \tag{16}$$

Here, g_{ML}^{hl} is the conductance for heat at the mine–leaf interface ($mol \cdot m^{-2} \cdot s^{-1}$). We assume that wind velocity within a mine is zero. Consequently, heat is conducted between a mine and adjacent leaf tissues through free convection mechanisms only. The conductance for heat at the mine–leaf interface in free convection is

$$g_{ML}^{hl} = 0.05 \left(\frac{T_M - T_L}{P_M} \right)^{0.25} \tag{17}$$

with P_M being the area of the mine–leaf interface (m^2). The mine–leaf interface is assumed here to be a rectangular flat surface for which the large length corresponds to the perimeter of the mine and the small length to the thickness of the leaf. The factor 0.05 results from the use of air properties (Campbell and Norman 1998).

The latent heat budget of a mine.—Latent heat lost by a mine when water vapor leaves the system is determined by

$$E = \lambda g_M^v \left[\frac{e_s(T_M) - e_a}{p_a} \right]. \tag{18}$$

Here g_M^v is the mine conductance for water vapor ($mol \cdot m^{-2} \cdot s^{-1}$) and $e_s(T_M)$ is the saturation water vapor pressure (Pa) at temperature T_M (°C). The term $e_s(T_M) - e_a$ corresponds to the water vapor pressure deficit of the mine (D_M: Pa). The relationship (Eq. 18) implies that the air inside the mine is near saturation for water vapor, as it is for the leaf internal atmosphere. This assumption is supported by the observation of water condensation inside the mine after a rapid drop in mine temperature (S. Pincebourde and J. Casas, *personal observation*). The saturation water vapor pressure $e_s(T_M)$ is determined by the Eq. 7 from the mine temperature. The conductance term g_M^v is computed from

$$g_M^v = \frac{0.5}{\frac{1}{g_M^{va}} + \frac{1}{g_M^{vs}}} + \frac{0.5}{\frac{1}{g_M^{va}} + \frac{1}{g_M^{ve}}} \tag{19}$$

where g_M^{va} is the mine boundary layer conductance, g_M^{vs} is the mine stomatal conductance, and g_M^{ve} is the upper mine epidermis conductance for water vapor. This equation is given for a hypostomatous leaf. Following the logic explained for the boundary layer conductance for heat, the mine boundary layer conductance for water vapor is expected to equal the leaf boundary layer conductance for water vapor, g_L^{va}, which is computed from Eq. 10. The model from Jarvis (1976) was used to determine the mine stomatal conductance:

$$g_M^{vs} = g_M^{smax} f_M^1(Q) f_M^2(D_M) f_M^3(T_M) \tag{20}$$

where g_M^{smax} is the maximal stomatal conductance of mined leaf tissues ($mol \cdot m^{-2} \cdot s^{-1}$), attained under specific levels of leaf irradiance (Q), mine water vapor pressure deficit (D_M: Pa) and mine temperature (T_M: °C). The functions f_M^1, f_M^2, and f_M^3 describe variations of stomatal conductance relative to the maximal value following a change in leaf irradiance, mine water vapor pressure deficit, and mine temperature, respectively.

The mine temperature calculation.—As for the computation of the leaf temperature, each term in Eq. 12 was replaced by its full expression. The thermal balance of the mine was expressed as a complex polynomial expression that was solved by an iterative process. The two models (leaf temperature and mine temperature) were combined in order to predict leaf and mine temperature from the driving variables air temperature, air relative humidity, and irradiance level. All driving variables and model parameters experimentally measured are given in Table 1. The changes in leaf tissues caused by the leaf miner were also quantified (see *Methods: Optical properties of intact leaves and mined*

TABLE 1. Values of the measured parameters and range of values for the driving variables used in the model.

Parameters	Symbols	Values (units)	Sources†
Climatic variables			
Air temperature	T_{air}	12–36°C	driving variable
Wind velocity	u	0.4–7 m/s	driving variable
Air relative humidity	hr	20–90%	driving variable
Irradiance (PAR)	Q	0–1600 $\mu mol \cdot m^{-2} \cdot s^{-1}$	driving variable
Global radiation	Rad	0–720 W/m^2	driving variable
Proportion of Rad in the VIS	I^{VIS}	37%	
Proportion of Rad in the NIR	I^{NIR}	63%	
Radiation budget			
VIS leaf absorbance	a_L^{VIS}	0.84	
NIR leaf absorbance	a_L^{NIR}	0.02	
VIS mine absorbance	a_M^{VIS}	0.48	
NIR mine absorbance	a_M^{NIR}	0.44	
Plant conductance, upper surface‡			
Upper leaf epidermis	g_L^{ve}	0.003 $mol \cdot m^{-2} \cdot s^{-1}$	Pincebourde et al.
Upper mine epidermis	g_M^{ve}	0.009 $mol \cdot m^{-2} \cdot s^{-1}$	Pincebourde et al.
Plant conductance, lower surface			
Leaf max. stomatal cond.	g_L^{smax}	0.274 $mol \cdot m^{-2} \cdot s^{-1}$	
Mine max. stomatal cond.	g_M^{smax}	0.227 $mol \cdot m^{-2} \cdot s^{-1}$	
Leaf stomatal response to Q	$f_L^1(Q)$	see Table 2	
Mine stomatal response to Q	$f_M^1(Q)$	see Table 2	
Leaf stomatal response to D_L	$f_L^2(D_L)$	see Table 2	
Mine stomatal response to D_M	$f_M^2(D_M)$	see Table 2	
Leaf stomatal response to T_L	$f_L^3(T_L)$	see Table 2	
Mine stomatal response to T_M	$f_M^3(T_M)$	see Table 2	
Metric parameters			
Leaf characteristic dimension	d_L	4.64×10^{-2} m	
Mine–leaf interface area	P_M	1.40×10^{-5} m^2	
Mine surface	S_M	1.02×10^{-4} m^2	

Notes: Key to abbreviations and variables: PAR, photosynthetically active radiation; VIS, visible; NIR, near infrared; max, maximal; D, water vapor pressure deficit; T_L, leaf temperature; T_M, mine temperature. Equations for the stomatal response functions are given in Table 2.

† Data are from the current study except as noted.

‡ Conductance values for the upper surfaces have been taken from S. Pincebourde, E. Frak, J. L. Regnard, H. Sinoquet, and J. Casas, *unpublished manuscript*.

leaf tissues, and also *Methods: Stomatal conductance of mines and intact leaves*).

Predicting the body temperature of larvae

We employed an empirical model to predict the body temperature of the leaf miner. Body temperature depends on (1) mine temperature, which is calculated by the biophysical model described above (see *Methods: The mine temperature model*), and (2) the amount of radiation transmitted by the upper mine epidermis that reaches the larva's body. Feeding windows transmit much more radiation than green patches (Pincebourde and Casas 2006). Therefore, body temperature depends on the position of larvae within the mine (i.e., positioned below feeding windows or green patches). The body temperature of a larva was computed from

$$T_{body} = T_M + f_{body}^k(Q) \quad (21)$$

where $f_{body}^k(Q)$ is the empirical function describing the body-to-mine temperature deviation as a function of leaf irradiance (Q) at the k position. This function is, for feeding windows (FW) and green patches (GP; Pincebourde and Casas 2006), as follows:

$$f_{body}^{FW} = (0.0034Q) + 0.0293 \quad (22)$$

$$f_{body}^{GP} = (0.0013Q) - 0.017. \quad (23)$$

These two functions, related to larval position within a mine, describe how much body temperature is warming compared to mine temperature under a given radiation level. These relationships were measured at a mine temperature of 25°C (Pincebourde and Casas 2006). We assumed that they are applicable to other mine temperatures because *P. blancardella* larvae are not able to thermoregulate physiologically. Indeed, for an insect with a small body size living in an environment nearly saturated for water vapor, evaporative cooling cannot be employed to decrease body temperature (Prange

1996). The mine habitat is saturated for water vapor regardless of the relative humidity in the ambient air (see *Methods: The mine temperature model: The latent heat budget of a mine*). A leaf miner larva cannot release the radiative energy it gains below the mine integument, inducing a linear relationship between the amount of radiation and the increase in body temperature.

Optical properties of intact leaves and mined leaf tissues

Optical properties of intact leaf tissues and mined leaf tissues were measured with a LI-1800 spectroradiometer coupled with a LI-1800-12 integrating sphere (Li-Cor, Lincoln, Nebraska, USA). This system records the amount of reflected and transmitted light from all directions (hemispherical, 180° solid angle) above the measured surface (1.77 cm^2 disc). Reflectance and transmittance of both lower and upper sides were scanned every 5 nm from 400 to 1100 nm on 10 intact leaves and 11 mines as in Combes et al. (2000).

The mine surface (~1 cm^2) was smaller than the 1.77 cm^2 disc of the LI-1800–12. Therefore, a large piece of white paper having a high reflectance (Kodak Premium Picture paper) was perforated to create a 0.72 cm^2 hole. This piece of paper was placed on the mine surface such that the hole was fully covered by mined leaf tissues. Reflectance and transmittance spectra of the white paper were measured as a control. The white paper reflected 92% and 93% of incident light in the visible (400–700 nm) and near infrared (800-1100 nm) spectra, respectively. It transmitted 4% and 7% of incident light in the visible and near infrared spectra, respectively. These small amounts of reflected and transmitted light by the white paper were taken into account for mine absorbance calculations.

Surface-averaged absorbance a at wavelength i was determined by

$$a_i = 1 - \left(\frac{R_i^{\text{upr}} + R_i^{\text{lwr}} + T_i^{\text{upr}} + T_i^{\text{lwr}}}{2} \right) \qquad (24)$$

(Combes et al. 2000), where R_i^{upr} and R_i^{lwr} are the portion of incident light reflected by the upper and lower surface at wavelength i, respectively, and T_i^{upr} and T_i^{lwr} are the portion of incident light transmitted by the upper and lower surface, respectively. The use of Eq. 24 implies that upper and lower leaf surfaces have a similar optical behavior. We therefore tested this assumption in both leaf and mined leaf tissues. Mean absorbance was obtained averaging all values of a_i in the visible range (400–700 nm) and in the near infrared range (800-1100 nm) for both intact leaf ($a_{\text{L}}^{\text{VIS}}$ and $a_{\text{L}}^{\text{NIR}}$) and mined leaf tissues ($a_{\text{M}}^{\text{VIS}}$ and $a_{\text{M}}^{\text{NIR}}$), respectively. Absorbance values were a straight average of all values in each range of wavelength, and were not weighted by using measurements of incoming solar radiation. Indeed, we assumed that the irradiance spectrum of ambient light is flat in the visible and near infrared ranges (but differed between the two ranges; see *Methods: Testing the models: Preparation of the climatic chamber*). For the simulation purposes, we assumed that absorbance in the range 1100–2500 nm equals that in the measured near infrared range 800-1100 nm. This assumption would not matter since there is so much incoming solar radiation from 1100 to 2500 nm (Campbell and Norman 1998).

Stomatal conductance of mines and intact leaves

The apple leaf is hypostomatous (i.e., stomata are restricted to the lower epidermis). The stomatal conductance responses to leaf irradiance (Q), vapor pressure deficit (D_{L} or D_{M}), and temperature (T_{L} or T_{M}) were studied in situ on both intact leaf tissues and mined leaf tissues. Gas exchanges were measured with an infrared gas analyzer–leaf chamber system (LI-6400, Li-Cor, Lincoln, Nebraska, USA), which allowed environmental variables within the leaf chamber (6-cm^2 area) to be controlled. Stomatal conductance (g_{L}^{vs} and g_{M}^{vs}: mol $H_2O \cdot m^{-2} \cdot s^{-1}$) was calculated by the LI-6400 data analysis program using the general gas exchange formula from von Caemmerer and Farquhar (1981). A light source with a 250-W metal iodide bulb (Sylvania Britelux HSI-T SX, clear) was used to illuminate the leaf surface. All measurements were made under standard conditions for the ambient CO_2 concentration (35 Pa; Le Roux et al. 1999). The leaf chamber enclosed a 6 cm^2 leaf surface, an area much larger than that of a mine. Thus, we coated the intact lower face of leaves with a thin layer of vegetable oil using a fine brush, leaving only the mined leaf tissues uncovered. Water vapor could therefore only be lost through mined leaf tissues. The vegetable oil efficiently inhibits gas exchanges and does not alter stomatal behavior of the uncovered surfaces (S. Pincebourde, E. Frak, J. L. Regnard, H. Sinoquet, and J. Casas, *unpublished manuscript*).

Stomatal conductance responses to climatic alterations.—All response curves were measured on different leaves. All mines were located on separate leaves containing no more than two mines, each mine being used only once. The responses of g_{L}^{vs} and g_{M}^{vs} ($mol \cdot m^{-2} \cdot s^{-1}$) to Q were measured on 5 intact leaves and 5 mines, respectively, according to 10 irradiance levels decreasing from 1500 to 0 $\mu mol \cdot m^{-2} \cdot s^{-1}$. The distance between the lamp and the sample was varied to attain different irradiance levels (from a maximal irradiance of 1600 $\mu mol \cdot m^{-2} \cdot s^{-1}$ at 20 cm from the lamp to an irradiance of 50 $\mu mol \cdot m^{-2} \cdot s^{-1}$ at ~150 cm from the lamp). The responses of g_{L}^{vs} and g_{M}^{vs} to increasing D_{L} were measured on 4 leaves and 4 mines (5 steps from 1 to 3 kPa), respectively. The effect of a variation in T_{L} on g_{L}^{vs} and g_{M}^{vs} was determined on 4 leaves and 4 mines (three steps from 19°C to 30°C), respectively. For each measurement, the two other variables were held at their reference value (i.e., temperature of 25°C, irradiance level of 1500 $\mu mol \cdot m^{-2} \cdot s^{-1}$ for intact leaves and 600 $\mu mol \cdot m^{-2} \cdot s^{-1}$ for mines, and water vapor pressure deficit of 1 kPa; Le Roux et al. 1999; S. Pincebourde, E. Frak,

J. L. Regnard, H. Sinoquet, and J. Casas, *unpublished manuscript*). All measurements were made on preilluminated leaves to ensure that stomata were active. An equilibration time of 20–30 min was imposed before any measurement. Measurements were discarded if stomatal conductance was not stable after 45 min. Leaves containing the measured mines were cut following the measurements and images of the lower mines surface were obtained using a scanner. Scans were analyzed using Scion Image software (Scion, Frederick, Maryland, USA) to measure mine areas in order to express stomatal conductance per unit of transpiring surface (i.e., mine surface; S. Pincebourde, E. Frak, J. L. Regnard, H. Sinoquet, and J. Casas, *unpublished manuscript*).

Leaf and mine maximal stomatal conductance.—Maximal stomatal conductance, g_L^{smax} and g_M^{smax} ($mol \cdot m^{-2} \cdot s^{-1}$), were measured under the conditions allowing the stomatal conductance to be at its highest value on 20 intact leaves ($T_L = 25$ °C, $Q = 1500$ $\mu mol \cdot m^{-2} \cdot s^{-1}$, and $D_L = 1$ kPa) and on 20 mines located on separate leaves containing no more than 2 mines ($T_M = 19$°C, $Q = 600$ $\mu mol \cdot m^{-2} \cdot s^{-1}$,and $D_M = 1$ kPa). All measurements were made on preilluminated leaves and a 20–30 min equilibration time was applied. Mined leaf tissue areas were measured using a scanner and the Scion Image software.

Test of the Jarvis hypothesis.—Changes in environmental parameters act independently from each other on the stomata opening level according to the Jarvis hypothesis. Predictions from Eqs. 11 and 20 were tested against independent measurements of stomatal conductance to test for the accuracy of the Jarvis hypothesis. An independent set of 19 intact leaves and 17 mines was used to measure first the maximal stomatal conductance (g_L^{smax} and g_M^{smax}) under the reference conditions (see *Methods: Stomatal conductance of mines and intact leaves: Stomatal conductance responses to climatic alterations*). Then two variables (irradiance level, leaf vapor pressure deficit, and/or leaf temperature) were altered such that the amplitude of the changes covered the interval of variation of these variables during stomatal conductance response measurements. All measurements were made on preilluminated leaves and a 20–30 min equilibration time was applied. Mined leaf tissue areas were measured using the same method. We incorporated the new values of the altered variables (irradiance level, leaf vapor pressure deficit, and leaf temperature) into Jarvis's Eqs. 11 and 20 to compare the Jarvis predictions to observed stomatal conductance.

Testing the models

Preparation of the climatic chamber.—Mine and leaf temperature were recorded within a 1.33-m^3 climatic chamber (VB 1014-A, Vötsch, Balingen Frommern, Germany) that allows for the control of relative humidity (hr, ±0.10% point) and air temperature (T_{air}, ±0.1°C). Inner walls of the chamber were made of synthetic PVDF (polyvinylidenfluoride) of "pure white" color RAL9010 with a thermal emissivity of 0.9. Two 250-W metal halide bulbs (Sylvania Britelux HSI-T SX clear) were fixed within the chamber, and irradiance level was altered by varying the distance between the sample and the lamps (lamps being fixed). The portion of total radiation emitted by the lamps in the visible and near infrared ranges was 0.37 and 0.63, respectively. The radiant flux incident to a surface at each point within the chamber was determined using (1) a pyranometer sensor (CM3, Campbell Scientific, Leicestershire, UK) connected to a CR10X data logger (Campbell Scientific) that recorded incident global radiation (Rad, W/m^2) from 305 to 2800 nm, and (2) a quantum sensor (LI-190SA, Li-Cor, Lincoln, Nebraska, USA) connected to a LI-1400 data logger that measured photosynthetically active radiation (Q: $\mu mol \cdot m^{-2} \cdot s^{-1}$) in the 400–700 nm waveband. The two sensors had a cosine corrected response allowing accurate measurements of flux densities through a plane surface. The simultaneous use of these two sensors gave us the possibility of converting the radiant flux from $\mu mol \cdot m^{-2} \cdot s^{-1}$ to W/m^2, and vice versa, for any measurements within the climatic chamber (linear regression, $W/m^2 = 0.4889$ $\mu mol \cdot m^{-2} \cdot s^{-1}$; $R^2 = 0.99$, $P < 0.001$, $N = 91$ measured points).

Wind velocity (u) within the ventilated chamber was measured with an air velocity transducer (Model 8465, TSI, St. Paul, Minnesota, USA) connected to a Campbell CR10X data logger. Wind velocity was spatially homogeneous within the working section of the chamber, which was located at least 30 cm from any wall. We verified that conditions for forced convection processes prevailed within the climatic chamber by calculating the ratio $Re^2 : Gr$, Re being the Reynolds number and Gr the Grashof number. Nobel (1999) consider that forced convection dominates when this ratio is higher than 10. The Reynolds number, Re, was computed from

$$Re = \frac{u d_L}{\nu} \tag{25}$$

where ν is the air kinematic viscosity ($\nu = 13.3 \times 10^{-6} \cdot m^{-2} \cdot s^{-1}$). The Grashof number, Gr, was determined using

$$Gr = \frac{g d_L^3 |T_L - T_{air}|}{T_{air} \nu^2} \tag{26}$$

where g is the gravity ($g = 9.8$ m/s), T_{air} is the air temperature (K), and $|T_L - T_{air}|$ the absolute value of the leaf to air temperature deviation.

Measurement of leaf and mine temperatures.—A set of 32 apple seedlings was chosen and one leaf per seedling was used for measurements of both mine and leaf temperature. Leaves were selected such that they were approximately similar age at the time of experiment

(30.2 ± 4.9 [mean ± SD] days, $N = 32$) and approximately similar width (6.45 ± 0.62 cm, $N = 32$). Each leaf had less than four mines (mean of 2.5 mines). During experiments, all leaves were forced to be perpendicular to the incident light flux by adequately orientating the petiole using wires. Selected mines were scanned and images were analyzed under Scion Image to measure their perimeter and to control for homogeneity in mine areas.

Leaf temperature was estimated as the average of two fine copper-constantan thermocouples (Type T, 0.2 mm diameter; TCSA, Dardilly, France) placed on the lower leaf surface, the first in the middle of the leaf and the second at its periphery, both being far from any mine. Mine temperature was measured by inserting a fine copper-constantan thermocouple (Type T) through a feeding window located on the upper mined leaf tissues. The insertion point was covered with vegetable oil in order to avoid any leak. All thermocouples (leaf and mine) were connected to a Campbell CR10X data logger placed outside the climatic chamber. We verified that the insertion method did not alter maximal stomatal conductance of the mine system on a further set of 29 mines. Measurements were taken with the LI-6400 infrared gas analyzer (see *Methods: Stomatal conductance of mines and intact leaves*) before and after insertion of a thermocouple through a feeding window and application of vegetable oil at mine temperature 25°C, irradiance 600 $\mu mol \cdot m^{-2} \cdot s^{-1}$, and mine vapor pressure deficit 1 kPa. A 25-min equilibration time was allowed before any measurement. There were no statistically significant differences in mine maximal stomatal conductance before insertion (0.117 ± 0.073 [mean ± SD] $mol \cdot m^{-2} \cdot s^{-1}$) and after insertion (0.123 ± 0.070 $mol \cdot m^{-2} \cdot s^{-1}$; $N = 29$, paired t test, $t_{28} = 0.66$, $P = 0.52$, NS).

Seedlings were placed within the climatic chamber. The temperature of each leaf and mine was measured under a different set of conditions of irradiance level (Q), air temperature (T_{air}), and air vapor pressure deficit (D_{air}), by keeping two parameters constant and varying the third. Relative humidity was adjusted in order to control for D_{air} (using Eqs. 7 and 8). Five leaves and 5 mines were measured at $T_{air} = 25$°C and $D_{air} = 1$ kPa (set A), and 5 other leaves and 5 other mines at $T_{air} = 19$°C and $D_{air} = 1$ kPa (set B). Leaf and mine temperatures were recorded at 7 irradiance levels (Q decreasing from 1300 to 0 $\mu mol \cdot m^{-2} \cdot s^{-1}$) for these two groups. Next, 4 leaves and 3 mines were measured at $Q = 1000$ $\mu mol \cdot m^{-2} \cdot s^{-1}$ and $D_{air} = 1$ kPa (set C), and 6 leaves and 4 mines at $Q = 400$ $\mu mol \cdot m^{-2} \cdot s^{-1}$ and $D_{air} = 1$ kPa (set D). In the two cases, leaf and mine temperatures were measured at 8 values of air temperature (from 12°C to 36°C). Finally, 7 leaves and 4 mines were placed at $Q = 1000$ $\mu mol \cdot m^{-2} \cdot s^{-1}$ and $T_{air} = 30$°C (set E), and 6 leaves and 6 mines at $Q = 400$ $\mu mol \cdot m^{-2} \cdot s^{-1}$ and $T_{air} = 30$°C (set F), while leaf and mine temperatures were recorded at 5 levels for D_{air} ranging from 1 to 3 kPa. For all sets, a minimum of 40 min equilibration time was imposed between each measurement. Leaf and mine temperatures were averaged over 10 measures taken every minute. All mines were dissected to ensure that larvae were still alive after experiments. At the end of all experiments, leaves were dissected in order to measure their thickness under a binocular camera. Leaf thickness was measured in the middle of the leaf, which corresponded to the usual mine location (Pottinger and LeRoux 1971). The combination of conditions for the six independent data sets (A to F) is shown in Fig. 2. Model predictions were compared to leaf and mine temperature measurements to test the validity of the models.

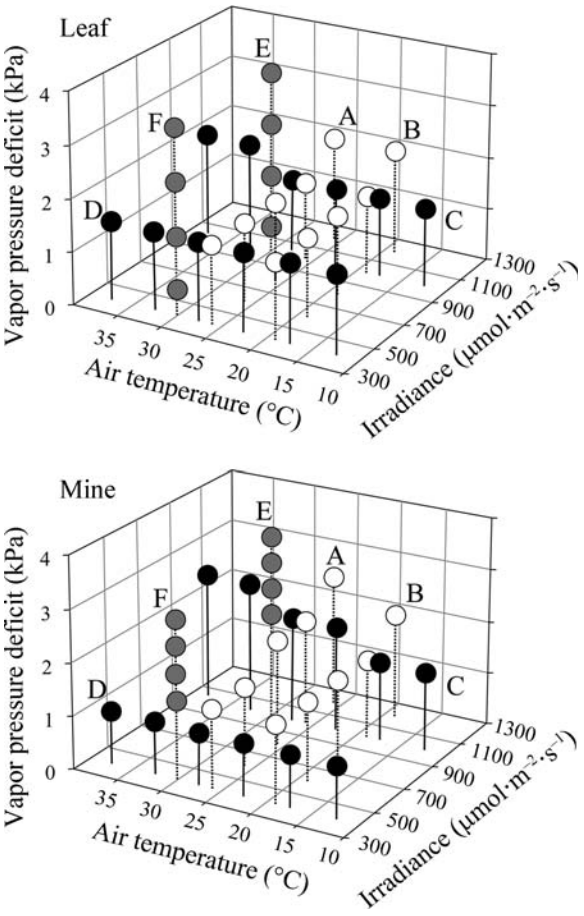

FIG. 2. Schematic representation of the experimental setup showing climatic conditions used for leaf and mine temperature measurements. Each set of data (A–F) is independent. The leaf and mine vapor pressure deficits were computed from the measured leaf and mine temperatures, the relative humidity, and using Eqs. 7 and 8. The shading of the different groups is only a visual aid.

Model simulations

Once the validity of the mine temperature model had been verified, the first step was to conduct simulations to identify the effect of a variation in each abiotic

parameter. In each simulation, one climatic parameter (radiation level, air temperature, relative humidity, or wind velocity) was varied while the others were held constant in order to quantify the impact of each variable on mine temperature. Secondly, we used two parameters to estimate the degree to which mine temperature was changing separately from leaf temperature (i.e., quantification of the degree of decoupling between mine and leaf microclimates): (1) the temperature difference between a mine and intact leaf tissues, and (2) the temperature excess of a mine when compared to ambient air. All other environmental parameters were held constant during these simulations. The third step was to simulate some situations that do not exist in nature, allowing us to distinguish the relative impact of insect-induced plant alterations on mine temperature (i.e., radiation absorption properties vs. stomatal conductance). Simulations of mine temperature were conducted using the parameters of both radiation absorption and stomatal behavior of the intact leaf, which corresponds to simulated virtual mines that do not alter plant tissues. This was obtained by replacing absorbance of the mine a_M^{VIS} and a_M^{NIR} by a_L^{VIS} and a_L^{NIR} in Eq. 14 and replacing in Eq. 20 the parameters $f_M^1(Q)$, $f_M^2(D_M)$, $f_M^3(T_M)$, and g_M^{smax} with $f_L^1(Q)$, $f_L^2(D_L)$, $f_L^3(T_L)$, and g_L^{smax}, respectively. This was used as an internal check of our model for a mine. Next, mine temperature was simulated using absorbance parameters of intact leaf tissues and stomatal conductance parameters of mined leaf tissues. This corresponds to virtual mines that only affect stomatal physiology.

Statistical analysis

The differences in optical properties between intact leaf tissues and mined leaf tissues were tested using a Mann-Whitney test. The stomatal conductance responses were analyzed under TableCurve 2D (SYSTAT, Chicago, Illinois, USA) employing nonlinear regressions, based on mechanistic models when possible, and performing least squares analysis (Johnson and Omland 2004). The difference in maximal stomatal conductance between leaves and mines was tested using a Student t test (two tailed) after having tested for the assumption of normal distribution of the data (Lilliefors probability test). The models were tested for their accuracy performing Pearson correlations between predictions and measurements and calculating the root mean square error (RMSE) of the predictions from the 1:1 relationship (i.e., measured temperature equals predicted temperature).

Results

Parameter estimation: optical properties

The mean absorbance of intact leaf tissues in the visible range ($a_L^{VIS} = 0.86 \pm 0.02$ [mean $\pm$ SD], $N = 10$) was higher than that in the near infrared (NIR) range ($a_L^{NIR} = 0.02 \pm 0.01$, $N = 10$; Mann-Whitney test, $P < 0.001$; Fig. 3A). By contrast, mined leaf tissues equally absorbed in the visible and NIR ranges ($a_M^{VIS} = 0.48 \pm 0.04$ and $a_M^{NIR} = 0.44 \pm 0.05$, respectively, $N = 11$; Mann-Whitney test, $P = 0.06$, NS; Fig. 3A). The mean absorbance of intact leaf tissues was higher than that of mined leaf tissues in the visible range (Mann-Whitney test, $P < 0.001$), but was lower in the NIR range (Mann-Whitney test, $P < 0.001$; Fig. 3A). The intact apple leaf had a high absorption in the blue (around 450 nm) and red (around 650 nm) wavelengths and a very low absorption in the NIR range (Fig. 3B). On the contrary, the absorption spectrum of mined leaf tissues appeared nearly flat from 500 to 1100 nm (Fig. 3B). For both leaves and mines, absorption spectra when receiving radiation from below were similar to that when radiation were incident to the upper surface (not shown), due to the complex trajectories followed by the light within a leaf and a mine.

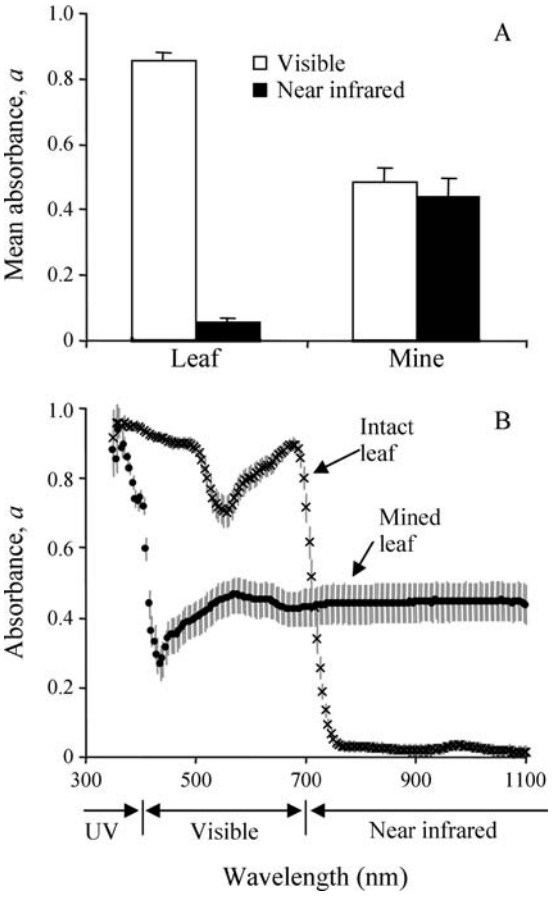

FIG. 3. Optical properties of leaf and mine tissues. (A) Mean absorbance (+SD) of intact leaf and mine tissues in the visible (white histograms) and near infrared (solid histograms) ranges. (B) Absorption spectrum of intact leaf (x's) and mined leaf tissues (solid circles) in the ultraviolet (UV), visible, and near infrared ranges. Gray bars indicate $\pm$SD.

Parameter estimation: stomatal conductance

The mean maximal stomatal conductance of mined leaf tissues (0.227 $\pm$ 0.108 mol·m^{-2}·s^{-1}, $N = 20$) was

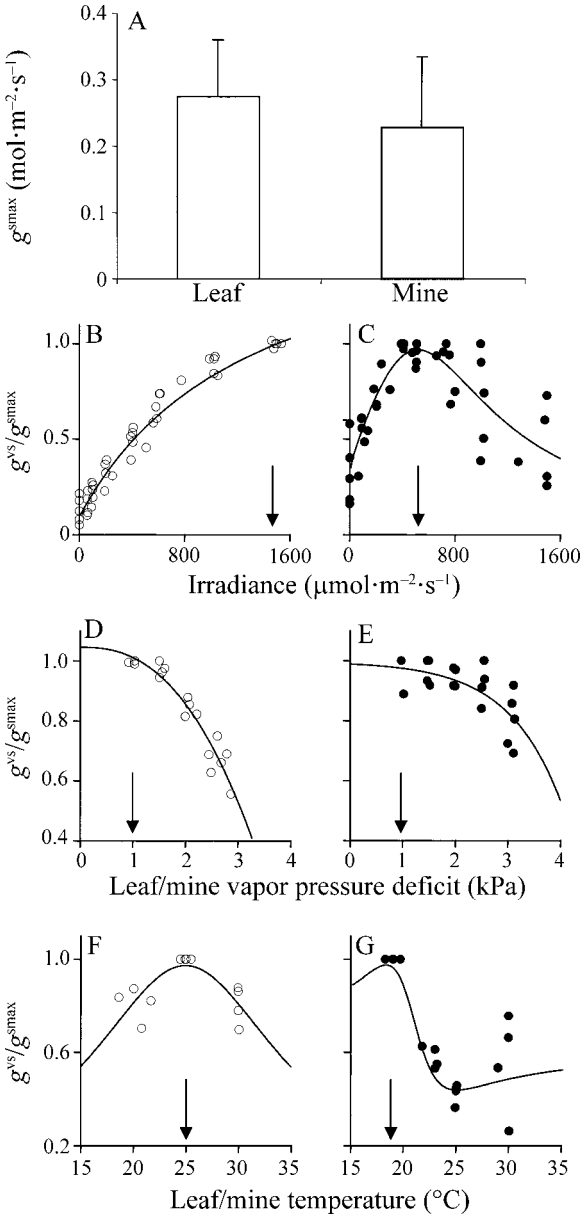

FIG. 4. Stomatal conductance parameters. (A) Maximal stomatal conductance (mean + SD) of intact leaf tissues (g_L^{smax}) and mined leaf tissues (g_M^{smax}). (B–G) Stomatal conductance responses of intact leaf tissues (open circles) and mined leaf tissues (solid circles) to a change in (B and C) irradiance, (D and E) leaf or mine vapor pressure deficit, and (F and G) leaf or mine temperature. The stomatal conductance was expressed relative to the maximal value shown in (A). All nonlinear regressions were significant (see Table 2 for statistics). Arrows on the *x*-axis show the values of each parameter used to measure maximal stomatal conductance.

similar to that of intact leaf tissues (0.274 ± 0.088 mol·m^{-2}·s^{-1}, $N = 20$; Student t test, $t_{2,19} = 1.29$, $P = 0.21$, NS; Fig. 4A). The stomatal conductance responses to irradiance, leaf water vapor pressure deficit, and temperature for both intact leaf tissues and mined leaf tissues were expressed relative to their maximal stomatal conductance level. Stomatal conductance increased with irradiance level in intact leaf tissues, whereas it increased at low irradiance levels but continuously decreased from moderate to high irradiance level in mined leaf tissues (Fig. 4B, C). Stomatal conductance strongly decreased from low to high levels of leaf vapor pressure deficit in intact leaf tissues. This decrease was weaker in mined leaf tissues (Fig. 4D, E). Stomatal conductance was maximal in intact leaf tissues at leaf temperature 25°C, whereas this maximum was found in mined leaf tissues at mine temperature 19°C (Fig. 4F, G). All nonlinear regressions were statistically significant (Table 2).

Validity of the models

The Jarvis hypothesis.—The predictions of the Jarvis hypothesis (Eqs. 11 and 20) were well matched by the independent measurements of stomatal conductance in both intact leaf tissues (Pearson's $r = 0.96$, $P < 0.001$, $N = 19$) and mined leaf tissues (Pearson's $r = 0.81$, $P < 0.001$, $N = 17$; Fig. 5). The root mean square error of prediction, RMSE, was 0.022 μmol·m^{-2}·s^{-1} for intact leaf tissues (corresponding to 8% of the maximal leaf stomatal conductance) and 0.027 μmol·m^{-2}·s^{-1} for mined leaf tissues (corresponding to 12% of the maximal mine stomatal conductance; Fig. 5).

The leaf temperature model.—Wind velocity within the climatic chamber was 0.4 m/s and the measured leaves had a mean characteristic dimension of $4.64 \times 10^{-2} \pm 0.45 \times 10^{-2}$ m (see Table 1). Under these conditions, the Re^2 : Gr (Reynolds number : Grashof number) ratio was higher than 10 for a leaf-to-air temperature deviation ranging from 0° to 10°C in absolute value. This ratio was similar at air temperature 12°C and 36°C (Fig. 6). This shows that forced convection prevailed under the experimental conditions. The model predictions for leaf temperature were well matched by the independent measurements made under set A to set F climatic conditions (Pearson's $r = 0.99$, $P < 0.001$, $N = 190$ measurements; Fig. 7). The RMSE of the whole data set (i.e., merging the six different data sets from Fig. 2) was 0.81°C. Therefore, the model accurately predicts leaf temperature from 12° to 42°C.

The mine temperature model.—The mean perimeter of mines was 5.09 ± 1.51 cm and the mean leaf thickness was 267 ± 25 μm, leading to a mean mine–leaf interface area (P_M) of 0.14 cm^2 (see Table 1). Mean mine surface was 1.02 ± 0.28 cm^2. The predictions of mine temperatures were well matched by the independent measurements made under conditions of set A to set F (Pearson's $r = 0.99$, $P < 0.001$, $N = 172$ measurements; Fig. 7). The RMSE of predictions calculated on the whole data set was 0.85°C.

Model exploration: influence of climatic variables on mine temperature

Influence of air temperature.—In the dark, leaves were predicted to be ~1.5–2°C colder than ambient air in a

TABLE 2. Statistics of the nonlinear models used to describe the relationships between stomatal conductance and irradiance (Q), water vapor pressure deficit (D), and temperature (T). The subscripts L and M refer to leaf and mine, respectively.

Relationship	Equation	Type	Parameters	Statistics
$f^1_L(Q)$	$y = \frac{a(x-c)}{b+(x-c)}$	hyperbolic saturation	$a = 1.79$ $b = 1249.53$ $c = -73.46$	$P < 0.001$ $R^2 = 0.96$ $F_{2,38} = 538.60$
$f^1_M(Q)$	$y = \frac{a+bx^{0.5}}{1+cx^{0.5}+dx}$	empirical equation	$a = 0.29$ $b = -5.95 \times 10^{-4}$ $c = -0.06$ $d = 1.34 \times 10^{-3}$	$P < 0.001$ $R^2 = 0.69$ $F_{3,36} = 31.19$
$f^2_L(D_L)$	$y = a + bx^c$	power equation	$a = 1.05$ $b = -0.03$ $c = 2.49$	$P < 0.001$ $R^2 = 0.90$ $F_{2,14} = 79.87$
$f^2_M(D_M)$	$y = a + be^x$	empirical equation	$a = 0.10$ $b = -0.01$	$P < 0.001$ $R^2 = 0.42$ $F_{1,17} = 16.14$
$f^3_L(T_L)$	$y = \frac{a}{1+\left(\frac{x-b}{c}\right)^2}$	Lorentzian equation	$a = 0.97$ $b = 25.01$ $c = 11.15$	$P = 0.03$ $R^2 = 0.36$ $F_{2,9} = 5.13$
$f^3_M(T_M)$	$y = \frac{a+bx+cx^2}{1+dx+ex^2}$	empirical equation	$a = 0.71$ $b = -0.06$ $c = 1.44\times10^{-3}$ $d = -0.09$ $e = 2.30\times10^{-3}$	$P < 0.001$ $R^2 = 0.81$ $F_{4,18} = 26.05$

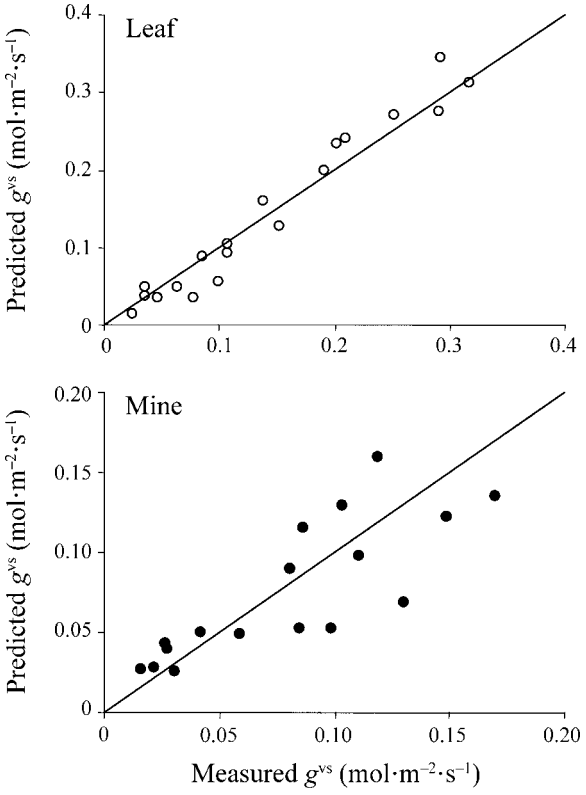

FIG. 5. Accuracy of the Jarvis hypothesis, shown by a comparison between independent measurements of stomatal conductance and predictions using the Jarvis hypothesis for intact leaf tissues (open circles) and mined leaf tissues (solid circles). Lines show the $x = y$ relationship. See *Results: Validity of the models: The Jarvis hypothesis* for statistics.

range of air temperature from 12° to 36°C (Fig. 8A). However, leaves were always warmer than ambient air at irradiance level above 600 μmol·m^{-2}·s^{-1}. The leaf-to-air temperature deviation was higher at air temperature 12°C than at 36°C, whatever the irradiance level (Fig. 8A). For example, at irradiance level 600 μmol·m^{-2}·s^{-1}, the leaf was ~2°C warmer than ambient at air temperature of 12°C, whereas it was near air temperature at 36°C (Fig. 8A). Nevertheless, at high irradiance level (1300 μmol·m^{-2}·s^{-1}), the evolution of the leaf-to-air temperature deviation as air temperature increased was

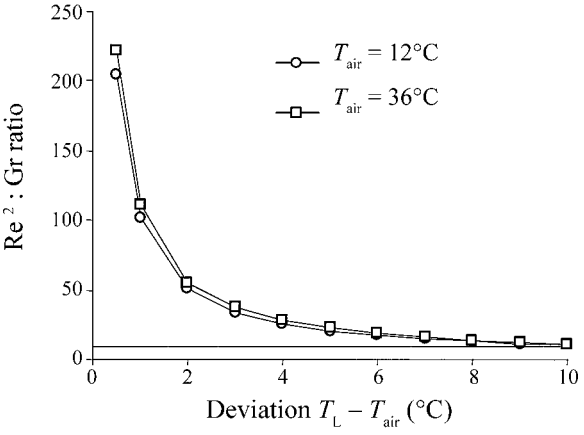

FIG. 6. Determination of the convection patterns within the climatic chamber using the relationship between the Re^2 : Gr (Reynolds number : Grashof number) ratio and leaf temperature excess at air temperature 12°C and 36°C. The horizontal line shows the threshold, at Re^2 : Gr = 10, above which forced convections are prominent.

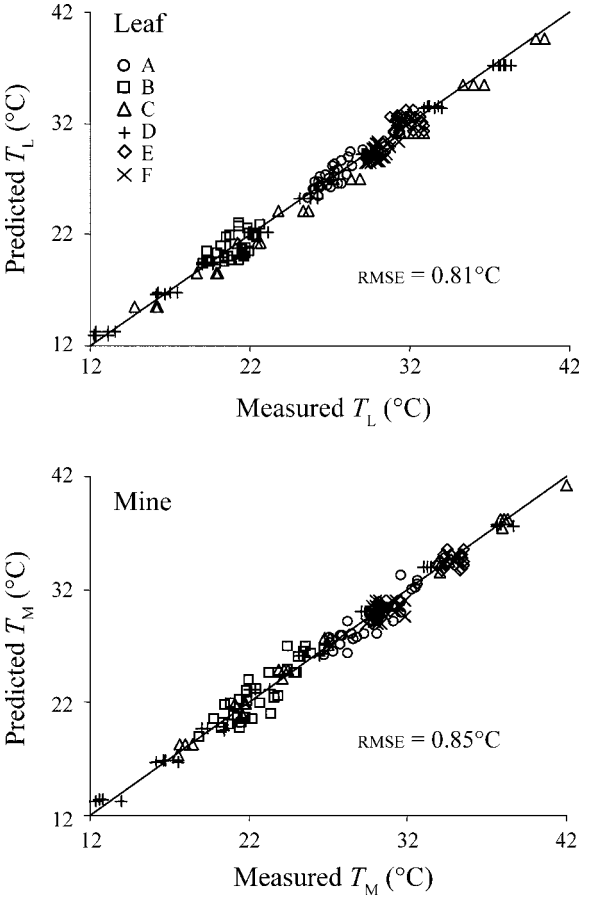

FIG. 7. Accuracy of leaf and mine temperature predictions as shown by a comparison between independent measurements of leaf and mine temperature and predictions of the temperature models. Experimental measurements were made under six different sets (A–F) of climatic conditions (see Fig. 2). Lines show the $x = y$ relationship, and the root mean square error (RMSE) was calculated on whole data sets.

U-shaped rather than continuously decreasing. The smallest deviation (~3.6°C above air temperature) was predicted at an air temperature of 25°C (Fig. 8A). By contrast, the mine-to-air temperature deviation was continuously decreased at all irradiance levels from air temperature 12°C to 36°C (Fig. 8B). For example, at irradiance level 950 $\mu mol \cdot m^{-2} \cdot s^{-1}$, the mine was 5.5°C warmer than ambient air at air temperature 12°C, whereas it was only 3.5°C above ambient air at 36°C (Fig. 8B). Therefore, the mine microclimate behaves differently to variations in air temperature than the leaf microclimate. This decoupling between mine and leaf temperatures resulted in a mine-to-leaf temperature deviation that varied over the air temperature range at a given irradiance level (Fig. 8C). For each irradiance level, the higher mine-to-leaf temperature deviation was obtained at air temperature ~20–25°C, whereas the lowest deviation was predicted at air temperature 36°C (Fig. 8C).

Influence of relative humidity.—The leaf temperature was predicted to increase as relative humidity increased at all irradiance levels and air temperature 25°C (Fig. 8D). A variation in relative humidity induced at best a change of ~2°C in leaf temperature at a given irradiance level. Similarly, the mine-to-air temperature deviation increased as air relative humidity increased and a variation in relative humidity induced at best a change of ~1.5°C in mine temperature (Fig. 8E). Therefore, relative humidity weakly altered the mine-to-leaf temperature deviation irrespective of irradiance level (Fig. 8F).

Influence of radiation level.—Highest variations in leaf and mine temperatures were predicted when radiation level was altered. As a general pattern, an increase in radiation level resulted in an increase in leaf-to-air and mine-to-leaf temperature deviation at a given air temperature and relative humidity (Fig. 8). A variation in radiation level could induce a change in mine-to-leaf temperature deviation of up to 5°C.

Effects of wind speed.—Mine and leaf temperatures decreased nonlinearly as wind speed increased (Fig. 9). At an irradiance level of 1600 $\mu mol \cdot m^{-2} \cdot s^{-1}$ and low velocities (i.e., $0 < u < 1$ m/s), a small change in wind speed induced a large temperature drop, whereas at high velocities (i.e., $u > 4$ m/s) a change in wind speed weakly affected mine and leaf temperatures (Fig. 9). The mine-to-leaf temperature deviation is also altered by wind speed. This deviation rapidly decreased at small wind velocities and was stabilized at high wind speed (Fig. 9).

Model exploration: influence of biotic parameters on mine temperature

Effects of plant-related modifications.—The leaf-to-air temperature deviation increased with irradiance at relative humidity 0.7 and air temperature 25°C (Fig. 10). At maximal irradiance level (1600 $\mu mol \cdot m^{-2} \cdot s^{-1}$) a leaf was 5.4°C warmer than the air. The temperature within the mine also increased but at a higher rate than that of the leaf (Fig. 10). At irradiance 1600 $\mu mol \cdot m^{-2} \cdot s^{-1}$ the mine was ~10°C hotter than the air and therefore ~5°C hotter than the leaf. The temperature of a virtual mine having nonaltered optical and stomatal properties was predicted to be much closer to leaf temperature at all irradiance levels, with a maximal deviation of 0.11°C (not shown). The temperature of a virtual mine with only altered stomatal physiology (i.e., optical properties of intact leaf tissues) was predicted to increase with irradiance level (Fig. 10). Modifications of the stomatal conductance responses lead to an increase of ~2°C at maximal irradiance level (Fig. 10). The observed changes in absorbance of mined leaf tissues induced the remaining increase, amounting to ~3°C at maximal radiation level.

Energy budgets.—The radiative, sensible, and latent heat budgets of a leaf (Eqs. 2, 3, and 6) and a mine (Eqs. 14, 15, 16, and 18) were computed as a function of

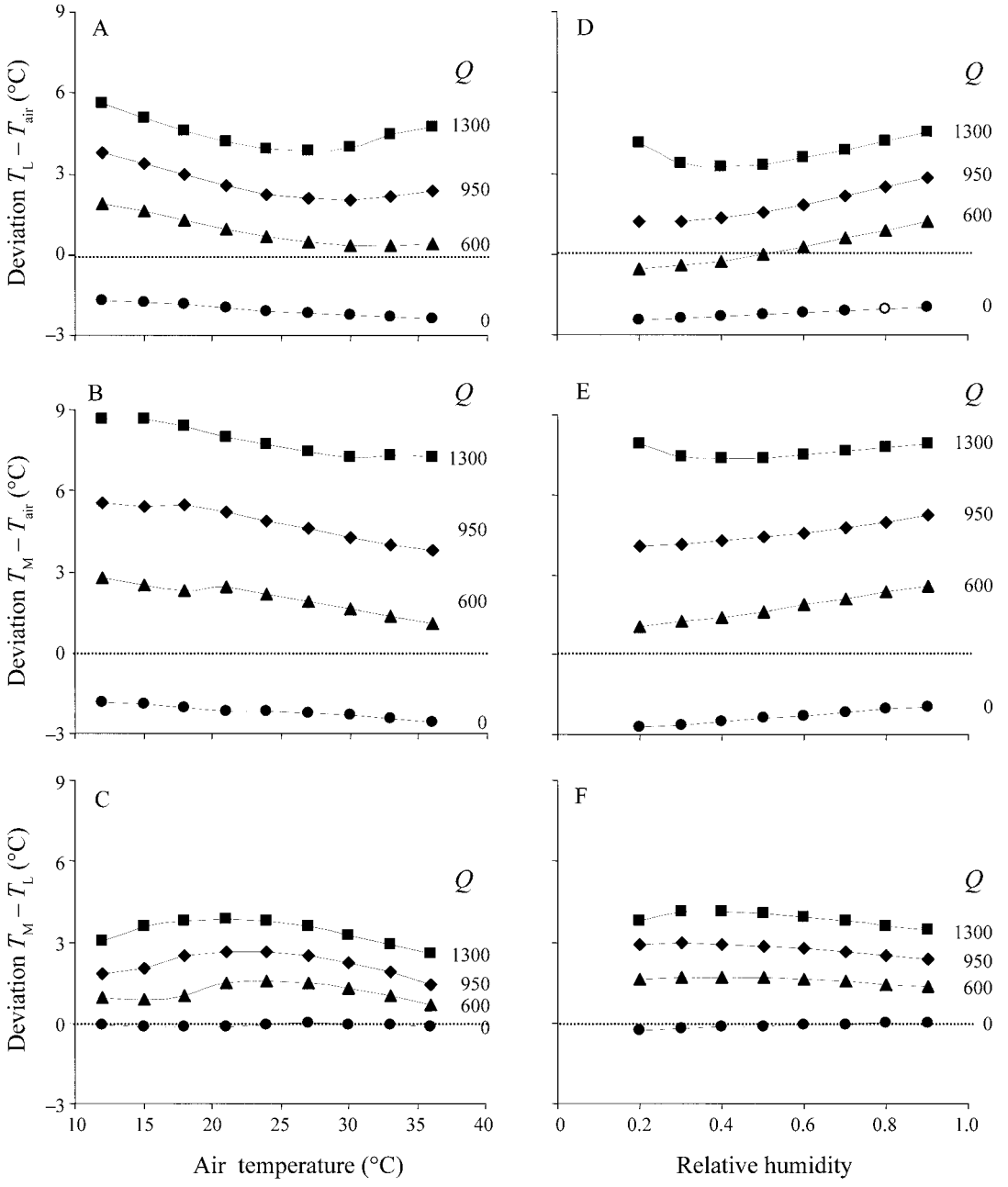

FIG. 8. Influence of climatic parameters on temperature predictions. (A–C) Temperature deviation between predicted leaf temperature (T_L), predicted mine temperature (T_M), and air temperature (T_{air}), as a function of air temperature at relative humidity of 0.7. (D–F) Temperature deviation between predicted leaf temperature, predicted mine temperature, and air temperature as a function of relative humidity at air temperature of 25°C. In each case, simulations were made at irradiance levels (Q) ranging from 0 to 1300 $\mu mol \cdot m^{-2} \cdot s^{-1}$.

radiation level at relative humidity 0.7 and air temperature 25°C. For any radiation level, the sum of the gain/loss was equal to zero in accordance to the Eq. 1. Both leaf and mine gained radiative heat as soon as the radiation level was above 90 W/m^2, a mine gaining always more radiative energy than a leaf (Fig. 11A). This was due to the fact that a mine absorbed more radiation than a leaf in the near infrared range (see Fig. 3). Both leaf and mine lost sensible heat as radiation level increased (Fig. 11B). The sensible heat loss of a mine was greater than that for a leaf mainly due to a large amount of heat exchanged with ambient air. The amount of heat exchanged with adjacent leaf tissues was weak. This is a consequence of (1) the high temperature

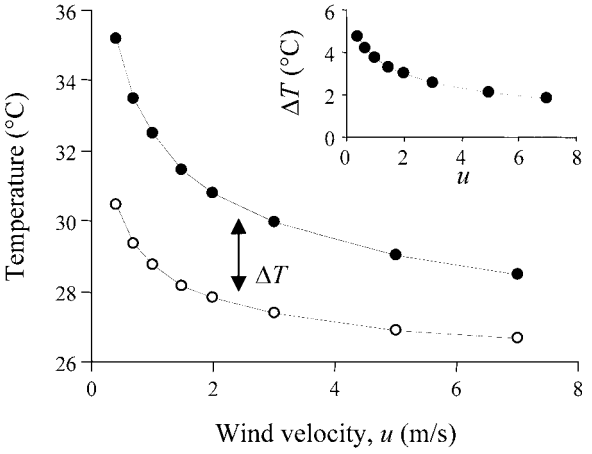

FIG. 9. Effect of wind velocity on leaf and mine temperature, showing predicted leaf and mine temperature as a function of wind velocity at irradiance of 1600 $\mu mol \cdot m^{-2} \cdot s^{-1}$ (780 W/m^2), air temperature of 25°C, and relative humidity of 0.7. The insert shows the mine-to-leaf temperature deviation (ΔT) as a function of wind velocity.

deviation between mines and ambient air, and (2) the small mine–leaf interface surface relative to the mine surface. Finally, both leaf and mine lost latent heat at all radiation levels. While a leaf lost an increasing amount of heat through transpiration with increasing radiation level, the latent heat loss of a mine remained constant from the moderate to the high radiation level (Fig. 11C). This was due to the light-dependent stomatal closure in mined leaf tissues (see Fig. 4).

Model exploration: larval body temperature

For a larva located below green patches or feeding windows, body-to-mine temperature deviation continuously increased with radiation level (Fig. 12). Body temperature of a larva located below green patches was 1°C warmer than mine temperature at high radiation level. Body temperature of a larva positioned below feeding windows, which transmit much more radiation than green patches (Pincebourde and Casas 2006), was up to 1.4°C above that of a larva below green patches at high radiation level (Fig. 12).

DISCUSSION

Assumptions and validity of the models

The biophysical model was quite robust and predicted leaf and mine temperature with a surprisingly high precision (near 0.8°C) in the range from 12°C to 42°C. Such a powerful mechanistic model is an appropriate tool to evaluate the impact of changes in the organism's physical environment on its body temperature. As is the case in any modeling work, several assumptions must be carefully considered when interpreting the model predictions.

The first assumption concerns the shape of the relationships describing the stomatal responses to leaf and mine water vapor deficits and to leaf and mine temperatures. These relationships were used beyond the range of data used to establish them (Fig. 4D–G). We extrapolated these relationships according to published studies that reported curves with similar shape within the range of values that we used (Jones 1992, Dang et al. 1997, Le Roux et al. 1999). For example, stomata in intact leaf tissues were shown to weakly respond to leaf water vapor deficit between 0 and 1 kPa (Jones 1992) and to rapidly close beyond 3 kPa (Jones 1992, Dang et al. 1997). By default, these extrapolations used in the leaf temperature model were also applied to the mine temperature model.

We found that the temperature of the intact portions of leaves infested by leaf miners was well predicted by the biophysical model of Campbell and Norman (1998) for an intact and noninfested leaf. This confirms that a mine corresponds to local modifications of plant tissues only. For example, the stomatal conductance and the transpiration rate in the intact leaf tissues adjacent to the mines are not affected by the presence of these mines (Proctor et al. 1982). The sensible heat transferred from the mine to the adjacent leaf tissues acted significantly to lower mine temperature under high radiation level. From the leaf point of view, however, this gain is negligible compared to the amount of sensible heat transferred from the leaf to ambient air. This is due to the small relative area of the mine–leaf contact surface that corresponds to only 0.58% of the total leaf surface.

The biophysical model assumes a spatially homogenous mean temperature over a full leaf. The model does not take into account the heterogeneity in the temperature distribution over a leaf surface, which is due to two phenomenon: (1) the stomatal patchiness that is a spatial and temporal heterogeneity in stomatal conductance over the leaf surface (e.g., Jones 1999, Mott and Buckley 2000), and (2) the aerodynamic cooling at the leading edges (e.g.,

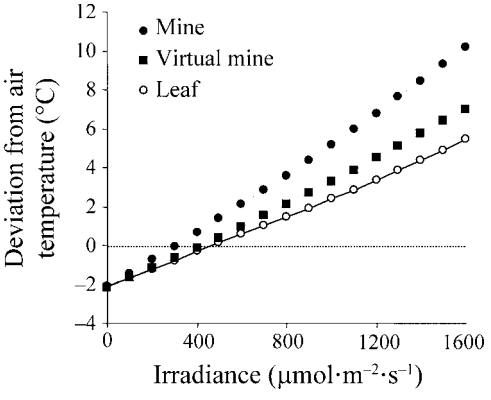

FIG. 10. Influence of biotic components on temperature predictions. The graph shows deviation between predicted temperature and air temperature as a function of irradiance level for a mine, a virtual mine that does not alter optical properties of plant tissues, and a leaf at air temperature of 25°C and relative humidity of 0.7.

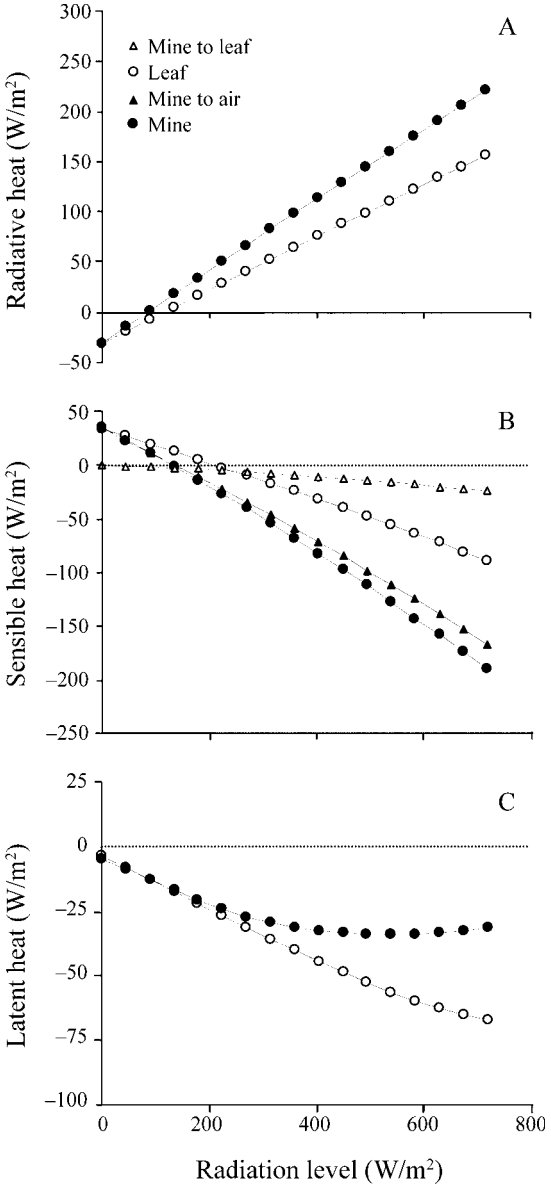

FIG. 11. Predicted (A) radiative, (B) sensible, and (C) latent heat budgets of a leaf (open circles) and a mine (solid circles) as a function of radiation level at air temperature of 25°C and relative humidity of 0.7. The sensible heat budget of a mine was split into sensible heat exchanged between a mine and ambient air (mine to air, solid triangles), and into sensible heat exchanged between a mine and adjacent leaf tissues (mine to leaf, open triangles). Positive values indicate heat gains, and negative values imply heat loss.

Roth-Nebelsick 2001). The temperature within a mine should therefore be best compared to the temperature of its host leaf precisely at the mine location. This cannot be done in reality, or with a model predicting a single mean leaf temperature. This assumption seems however reasonable considering the accuracy of model predictions. Our explanation is that the mined leaf area is probably disconnected from the stomatal patchiness occurring in the intact leaf portions, and mines are rarely found at the leaf margins, which are the colder leaf regions.

The biophysical model also assumes that a mine is a flat surface. This assumption allows us to simplify the calculations of boundary layer conductance for both heat and water vapor transfers. However, the upper mine surface is bulging, not flat. This protuberance may decrease the boundary layer thickness above the mine, leading to increasing heat loss through conductance and convection mechanisms. However, this protuberance (<3 mm in height) is certainly within the leaf boundary layer at low wind velocity. Furthermore, the leaf boundary layer is thinner at the upwind or leading edge and thicker in the center of a leaf (Nobel 1999). Mines were most frequently located in the center of the leaves (Pottinger and LeRoux 1971; S. Pincebourde, *personal observation*).

Feedback loops between biotic and abiotic parameters

Radiation level, air temperature, and wind speed are the major abiotic factors that affect the thermal environment of a leaf miner. Wind speed is certainly the more temporally heterogeneous parameter in the field, with variations between 0 and 3 m/s at the second scale (S. Pincebourde, *unpublished data*). Mine temperature decreases by ~5°C while wind speed is increasing from 0.4 to 3 m/s at high radiation level (Fig. 9). An increase in air temperature significantly leads to a warmer mine though the relationship is not strictly linear (i.e., the mine-to-air temperature deviation is ~2°C lower at air temperature 36°C than at 12°C; Fig. 8B). The effect of a change in radiation level is more striking. An elevation of the radiation level from zero to maximal level causes a change in mine temperature of

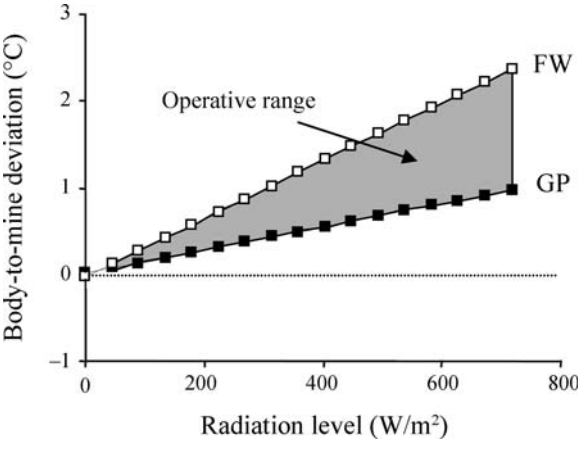

FIG. 12. Body-to-mine temperature deviation as a function of radiation level, for a larva located below feeding windows (FW, open squares) and below green patches (GP, solid squares) at air temperature of 25°C and relative humidity of 0.7. The operative body temperature range (gray section; i.e., the expected body temperature of a larva within the mine) is a function of its position relative to feeding windows.

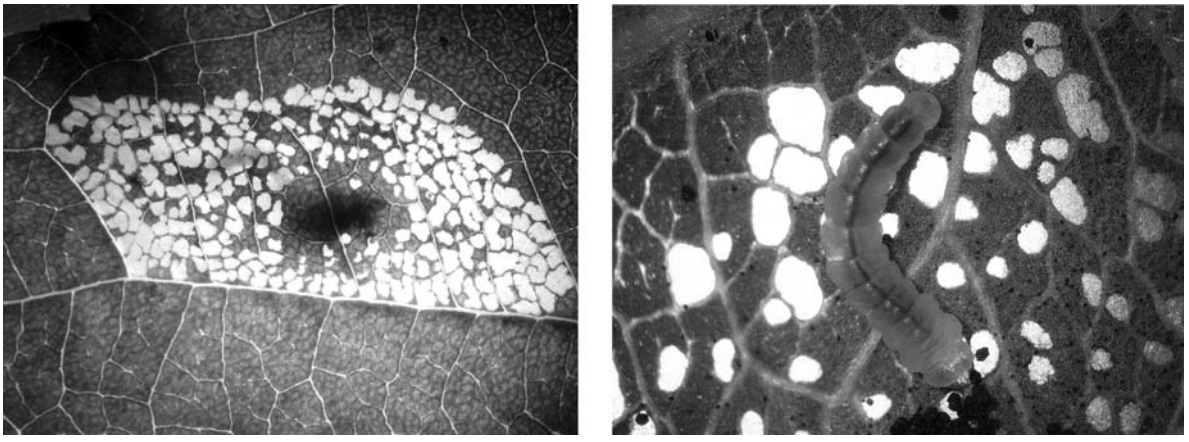

PLATE 1. Microhabitat of the leaf-mining moth *Phyllonorycter blancardella*. The larva develops inside the apple leaf tissues, within a structure called a mine (representing a surface of ~1 cm^2). (Left) A mine seen from the top. The caterpillar creates feeding windows (white areas) by feeding on the chlorophyll-containing plant tissues; the larva can be seen through the feeding windows when lighting the mine from below (in gray, below feeding windows). The larva leaves a relatively large area of intact plant tissues (green shield), below which feces are accumulating (black area in the middle of the green shield). (Right) Photograph taken after removing the lower mine integument which contains stomata. The larva (~3 mm long) is walking on the ceiling of its mine, which appears as a mosaic of feeding windows and green patches. The modifications provided by the larva to plant tissues cause a large temperature excess within the mine, of up to 10°C above ambient. Moreover, feeding windows transmit solar radiation within the mine, and the larva can lower its body temperature by resting below the green shield. The microclimatic conditions experienced greatly differ between leaf miners and insects resting at the leaf surface, even if only a few millimeters are separating the two animals. Photo credits: S. Pincebourde.

~12°C and body temperature is up to 14.5°C warmer under full radiation level than in the dark (Fig. 12). This impressive effect of radiation level is generated by the feedback loop between this abiotic factor and the biotic components of the system. From a biophysical point of view, radiation level acts on two distinct processes: (1) absorption of radiative heat, and (2) loss of latent heat (opening level of stomata). The leaf miner *P. blancardella* alters these two functions: absorbance properties are highly modified (Fig. 3) and stomatal behavior is altered (Fig. 4) in mine tissues. The two effects alter mine temperature independently and significantly. About 40% of the mine temperature excess was caused by stomatal closure while changes in absorbance properties contributed to 60% of this excess (Fig. 10). Indeed, the observed modifications in absorbance properties cause mines to gain much more radiative heat than leaves due to a greater absorbance of the former in the near infrared range (Fig. 11A). Moreover, latent energy is retained within mines in the higher radiation levels, when the opening level of stomata in mined leaf tissues is very small (Fig. 11C). The modifications provided by a larva to its biotic environment (i.e., plant tissues) induce changes in the effects of the abiotic parameters (i.e., radiation level) on the microclimate.

The modifications in absorbance properties directly result from the feeding activity of the larva. Its feeding behavior is highly organized and meticulous, resulting in the creation of feeding windows (Djemai et al. 2000, Pincebourde and Casas 2006). The shift in stomatal behavior in mined leaf tissues is a response to both mine morphology and the CO_2 released by the larva within the mine (S. Pincebourde, E. Frak, J. L. Regnard, H. Sinoquet, and J. Casas, *unpublished manuscript*). Therefore, modifications of plant tissues are directly linked to the activity of the larva within the mine. Larvae can therefore modulate the feedback loop between the biotic components (plant tissue properties) and the abiotic factors (radiation level) by altering their behavior.

The leaf miner's thermal environment: profitable but risky?

A mine acts as a little greenhouse with a highly efficient heating system (a mine absorbs more radiation than a leaf) and with a checked evaporative cooling system (a mine loses less latent heat than a leaf) (see Plate 1). Clearly, a mine is always warmer than a leaf during the day. Assuming that mine temperature is below the lethal threshold, an ectothermic organism directly benefits from this warm microclimate. In the dark, the temperatures of a mine and a leaf are not different, even under hot air temperature (Fig. 8). Therefore, a mine does not work as a buffer against extreme conditions. Instead, it enables herbivorous insects to decouple themselves from the microclimate of their host plant in order to gain extra heat when needed. However, this strategy seems risky at high radiation level and under extreme air temperature corresponding to conditions of clear sky during summer in Tours, France. The maximal air temperature at Tours (47°27′ N, 0°43′ E) during July and August, averaged

along the period 1951–2002, is 34°C (F. Decker, climatic database, *available online*).[2] Under these conditions, the mine-to-air temperature deviation was lowered so that the mine-to-leaf temperature deviation remains low under such extreme conditions (Fig. 8). Therefore, the internal working of a mine differs strikingly from that of a leaf, and allows the leaf miner to control for overheating. This ability prevents mines from attaining upper lethal temperature.

Moreover, our results indicate that the design of the mine offers the possibility for larvae to thermoregulate behaviorally. Larvae cannot thermoregulate physiologically (i.e., to enhance or decrease their body temperature, independently from the conditions, by metabolic means). Instead, body temperature is driven by mine temperature and radiation transmitted within the mine by the upper mine epidermis. A large area occupied exclusively by green patches is present at the center of the mine (Djemai et al. 2000; see Fig. 1A). At high radiation level, a larva could decrease its body temperature by ~1.5°C when moving from under feeding windows to green patches. This deviation can be of crucial importance to avoid lethal temperatures. Indeed, during extreme conditions of hot air temperature (34°C) and high radiation level (e.g., 580 W/m^2), body temperature is ~43.3°C for a larva below feeding windows and 41.9°C for a larva below green patches. The upper lethal temperature of last-instar *P. blancardella* larvae is 42°C (S. Pincebourde, *unpublished data*). Klok et al. (2003) also report a lethal temperature of 42°C in another leaf miner species. Behavioral experiments are now needed to test whether leaf miners really exploit the potentialities offered by the mine design.

Evolutionary ecology of the leaf-mining habit

Most leaf-mining insects develop within their mine until adult emergence. The intimate relationship between leaf miners and their host plants evolved over a long period of time and shows a high specificity (Lopez-Vaamonde et al. 2003). The leaf-mining habit is ancient and at least three subfamilies of *Gracillariidae* existed at the Early/Late Cretaceous boundary when Angiosperm radiation was still occurring (Labandeira et al. 1994). Here we provide the first evidence that the mine is built in such a way as to offer a life in a warmer environment than insects living at air temperature or leaf temperature can have. As long as upper lethal temperatures are not attained, the metabolic rate of the larvae is enhanced due to the temperature excess, leading to increased developmental rate. The developmental rates of last-instar larvae and pupae of *P. blancardella* increase linearly with temperature (Baumgartner and Severini 1987). A faster development can be viewed as a strategy to minimize the risk of attack by a parasitoid. Indeed, the shorter the developmental time, the lower the risk of being detected by a parasitoid according to the slow-growth-high-mortality hypothesis (Benrey and Denno 1997). This hypothesis remains however to be tested on a leaf-mining insect.

Additionally, several nonmutually exclusive hypotheses have been proposed to explain the adaptive significance of the leaf-mining habit (all reviewed in Connor and Taverner [1997]). First, being enclosed within mines, larvae might escape from natural enemies. Leaf-mining insects suffer a relatively lower mortality rate from pathogens and generalist predators in comparison to external feeding guilds. However, specialist parasitoids induce a higher mortality rate in the leaf miner feeding guild than in the external feeding guild (Connor and Taverner 1997, Hawkins et al. 1997). Second, leaf mining may be a strategy to avoid plant defenses or layers of leaf tissues having a low nutritional value. Many leaf miner species concentrate their feeding on the most nutritious leaf tissue, which is also the tissue with the lower structural defense content (Scheirs et al. 2001). The third main adaptive hypothesis is that the mine could protect larvae from the physical environment. The leaf miner *P. blancardella* is relatively protected from harmful ultraviolet radiation since both feeding windows and green patches only weakly transmit ultraviolet radiation inside a mine (Pincebourde and Casas 2006). Ultraviolet protection was also demonstrated in four other leaf miner species (Connor and Taverner 1997). Thus, our work adds a substantial body of understanding to the hypothesis of physical protection and interaction with climatic conditions in general.

Multitrophic biophysical heat budgets

Our work is the first to establish a complete heat budget for an herbivore insect–plant interaction. Our results show that the second trophic level manages and partially controls the first one, which in turn provides the insect with a modified thermal environment, even to the point of one trophic partner co-opting the physiology of the other. These reciprocal influences imply that heat budgets cannot be simply built for each trophic level independently. The integration of several trophic levels within a unique biophysical heat budget offers numerous possibilities. First, this approach allows us to identify and to quantify the feedback loops between climatic parameters and biotic factors. The control of abiotic parameters through the biotic environment within a single trophic level is not new (e.g., Helmuth 1998). Here we show that these feedback loops are of high importance in herbivore insect–plant interactions and that herbivores can modify plant tissues in order to amplify and control the effects of abiotic factors on their microclimate. Second, multitrophic heat budgets propose some perspectives in evolutionary ecology, and their interpretation would help to explain the evolution of some herbivore insect guilds. Finally, this model can now be extended to the third trophic level, parasitoids,

[2] ⟨http://www.lameteo.org/⟩

as they are living in the thermal environment created by the herbivore. Such a tritrophic biophysical model would be a powerful tool with which to study the dynamics of populations in a highly variable climatic environment, as is the case in the field.

Recently, Helmuth et al. (2005) advocated for the inclusion of physiological insight when predicting the effects of climate change on populations and ecosystems and suggested that the biophysical approach is a powerful tool for determining how organisms would be affected by changes in their physical environment. Such an approach highlights the difficulty of predicting the response of multitrophic interactions to climate changes, and our study is an important step in that direction. The stability of multitrophic interactions is indeed profoundly affected by perturbations in synchronicity, which is markedly affected by changes in temperature, as shown both theoretically and in the field (Hassell et al. 1993, Ives and Gilchrist 1993, Harrington et al. 1999, Edwards and Richardson 2004). Given the amplitude of expected climatic changes, multitrophic heat budgets as proposed here are the natural bridge between physiological ecology and population ecology necessary to explore the biotic consequences of the future climate changes.

Acknowledgments

We are grateful to Didier Combes, Eric Thibout, Claudio Lazzari, and Frédéric Decker for providing us with some of the materials; Christelle Magal and Hervé Sinoquet for helpful discussions about the model; Brian Helmuth, Olivier Dangles, David Giron, Johann Baumgärtner, Scott Turner, and an anonymous referee for comments on earlier versions of the manuscript. This study was mainly funded by a Ph.D. scholarship from the French Ministry for Education and Research to S.P. and by the ACI "Ecologie Quantitative" project "Ecologie Physique" led by J.C.

Literature Cited

Baumgartner, J., and M. Severini. 1987. Microclimate and arthropod phenologies: the leaf miner *Phyllonorycter blancardella* F. (Lep) as an example. Pages 225–243 *in* F. Prodi, F. Rossi, and F. Cristoferi, editors. International Conference on Agrometeorology, Cesena, Italy.

Benrey, B., and R. F. Denno. 1997. The slow-growth-high-mortality hypothesis: a test using the cabbage butterfly. Ecology **78**:987–999.

Campbell, G. S., and J. M. Norman. 1998. Plants and plant communities. Pages 223–246 *in* G. S. Campbell and J. M. Norman, editors. An introduction to environmental biophysics. Springer Verlag, New York, New York, USA.

Casey, T. M. 1992. Biophysical ecology and heat exchange in insects. American Zoologist **32**:225–237.

Combes, D., H. Sinoquet, and C. Varlet-Grancher. 2000. Preliminary measurements and simulation of the spatial distribution of the morphogenetically active radiation (MAR) within an isolated tree canopy. Annals of Forest Science **57**:497–511.

Connor, E. E., and M. P. Taverner. 1997. The evolution and adaptive significance of the leaf-mining habit. Oikos **79**:6–25.

Dang, Q. L., H. A. Margolis, M. R. Coyea, M. Sy, and G. J. Collatz. 1997. Regulation of branch-level gas exchange of boreal trees: roles of shoot water potential and vapor pressure difference. Tree Physiology **17**:521–535.

Danks, H. V. 2002. Modification of adverse conditions by insects. Oikos **99**:10–24.

Djemai, I., R. Meyhöfer, and J. Casas. 2000. Geometrical games between a host and a parasitoid. American Naturalist **156**:257–265.

Edwards, M., and A. J. Richardson. 2004. Impact of climate change on marine pelagic phenology and trophic mismatch. Nature **430**:881–884.

Gates, D. M. 1980. Biophysical ecology. Dover Publications, New York, New York, USA.

Gilbert, N., and D. A. Raworth. 1996. Insects and temperature—a general theory. Canadian Entomologist **128**:1–13.

Goldsbrough, C. L., D. F. Hochuli, and R. Shine. 2004. Fitness benefits of retreat-site selection: spiders, rocks, and thermal cues. Ecology **85**:1635–1641.

Grant, B. W., and W. P. Porter. 1992. Modeling global macroclimatic constraints on ectotherm energy budgets. American Zoologist **32**:154–178.

Harrington, R., I. Woiwod, and T. Sparks. 1999. Climate change and trophic interactions. Trends in Ecology and Evolution **14**:146–150.

Hassell, M. P., H. C. J. Godfray, and H. N. Comins. 1993. Effects of global change on the dynamics of insect host–parasitoid interactions. Pages 402–423 *in* P. M. Kareiva, J. G. Kingsolver, and R. B. Huey, editors. Biotic interactions and global change. Sinauer Associates, Sunderland, Massachusetts, USA.

Hawkins, B. A., H. V. Cornell, and M. E. Hochberg. 1997. Predators, parasitoids, and pathogens as mortality agents in phytophagous insect populations. Ecology **78**:2145–2152.

Helmuth, B. S. T. 1998. Interdidal mussel microclimates: predicting the body temperature of a sessile invertebrate. Ecological Monographs **68**:51–74.

Helmuth, B. S. T. 2002. How do we measure the environment? Linking intertidal thermal physiology and ecology through biophysics. Integrative and Comparative Biology **42**:837–845.

Helmuth, B., J. G. Kingsolver, and E. Carrington. 2005. Biophysics, physiological ecology, and climate change: Does mechanism matter? Annual Review of Physiology **67**:177–201.

Herrera, C. M. 1995. Floral biology, microclimate, and pollination by ectothermic bees in an early-blooming herb. Ecology **76**:218–228.

Huey, R. B. 1991. Physiological consequences of habitat selection. American Naturalist **137**:S91–S115.

Huey, R. B., and J. G. Kingsolver. 1989. Evolution of thermal sensitivity of ectotherm performance. Trends in Ecology and Evolution **4**:131–135.

Ives, A. R., and G. Gilchrist. 1993. Climate change and ecological interactions. Pages 121–146 *in* P. M. Kareiva, J. G. Kingsolver, and R. B. Huey, editors. Biotic interactions and global change. Sinauer Associates, Sunderland, Massachusetts, USA.

Jarvis, P. G. 1976. The interpretation of the variations in leaf water potential and stomatal conductance found in canopies in the field. Philosophical Transactions of the Royal Society of London Series B **273**:593–610.

Johnson, J. B., and K. S. Omland. 2004. Model selection in ecology and evolution. Trends in Ecology and Evolution **19**: 101–108.

Jones, H. G. 1992. Stomata. Pages 131–162 *in* H. G. Jones, editor. Plants and microclimate: a quantitative approach to environmental plant physiology. Cambridge University Press, Cambridge, UK.

Jones, H. G. 1999. Use of thermography for quantitative studies of spatial and temporal variation of stomatal conductance over leaf surfaces. Plant, Cell and Environment **22**:1043–1055.

Kingsolver, J. G. 2000. Feeding, growth, and thermal environment of cabbage white caterpillars, *Pieris rapae* L. Physiological and Biochemical Zoology **73**:621–628.

Kingsolver, J. G., and R. J. Moffat. 1982. Thermoregulation and the determinants of heat transfer in *Colias* butterflies. Oecologia **53**:27–33.

Klok, C. J., S. L. Chown, and K. J. Gaston. 2003. The geographical range structure of the holly leaf-miner. III. Cold hardiness physiology. Functional Ecology **17**:858–868.

Labandeira, C. C., D. L. Dilcher, D. R. Davis, and D. L. Wagner. 1994. Ninety-seven million years of angiosperm–insect association: paleobiological insights into the meaning of coevolution. Proceedings of the National Academy of Science USA **91**:12 278–12 282.

Lactin, D. J., and D. L. Johnson. 1998. Environmental, physical, and behavioural determinants of body temperature in grasshopper nymphs (Orthoptera: Acrididae). Canadian Entomologist **130**:551–577.

Layne, J. R. J. 1993. Winter microclimate of goldenrod spherical galls and its effects on the gall inhabitant *Eurosta solidaginis* (Diptera: Tephritidae). Journal of Thermal Biology **18**:125–130.

Le Roux, X., S. Grand, E. Dreyer, and F. A. Daudet. 1999. Parameterization and testing of a biochemically based photosynthesis model for walnut (*Juglans regia*) trees and seedlings. Tree Physiology **19**:481–492.

Lopez-Vaamonde, C., H. C. J. Godfray, and J. M. Cook. 2003. Evolutionary dynamics of host-plant use in a genus of leaf-mining moths. Evolution **57**:1804–1821.

Mott, K. A., and T. N. Buckley. 2000. Patchy stomatal conductance: emergent collective behavior of stomata. Trends in Plant Science **5**:258–262.

Nobel, P. S. 1988. Environmental biology of agaves and cacti. Cambridge University Press, New York, New York, USA.

Nobel, P. S. 1999. Physicochemical and environmental plant physiology. Second edition. Academic Press, New York, New York, USA.

O'Connor, M. P. 1999. Physiological and ecological implications of a simple model of heating and cooling in reptiles. Journal of Thermal Biology **24**:113–136.

O'Connor, M. P., and J. R. Spotila. 1992. Consider a spherical lizard: animals, models, and approximations. American Zoologist **32**:179–193.

Orueta, D. 2002. Thermal relationships between *Calendula arvensis* inflorescences and *Usia aurata* bombyliid flies. Ecology **83**:3073–3085.

Patiño, S., E. A. Herre, and M. T. Tyree. 1994. Physiological determinants of *Ficus* fruit temperature and implications for survival of pollinator wasp species: comparative physiology through an energy budget approach. Oecologia **100**:13–20.

Pincebourde, S., and J. Casas. 2006. Leaf miner-induced changes in leaf transmittance cause variations in insect respiration rates. Journal of Insect Physiology **52**:194–201. [doi:10.1016/j.jinsphys.2005.10.004]

Pottinger, R. P., and E. J. LeRoux. 1971. The biology and the dynamics of *Lithocolletis blancardella* (Lepidoptera: Gracillariidae) on apple in Quebec. Memoirs of the Entomological Society of Canada, Ottawa. Volume 77.

Prange, H. D. 1996. Evaporative cooling in insects. Journal of Insect Physiology **42**:493–499.

Pringle, R. M., J. K. Webb, and R. Shine. 2003. Canopy structure, microclimate, and habitat selection by a nocturnal snake, *Hoplocephalus bungaroides*. Ecology **84**:2668–2679.

Proctor, J. T. A., J. M. Bodnar, W. J. Blackburn, and R. L. Watson. 1982. Analysis of the effects of the spotted tentiform leafminer (*Phyllonorycter blancardella*) on the photosynthetic characteristics of apple leaves. Canadian Journal of Botany **60**:2734–2740.

Rombough, P. 2003. Modelling developmental time and temperature. Nature **424**:268–269.

Roth-Nebelsick, A. 2001. Computer-based analysis of steady-state and transient heat transfer of small-sized leaves by free and mixed convection. Plant, Cell and Environment **24**:631–640.

Ruf, C., and K. Fiedler. 2000. Thermal gains through collective metabolic heat production in social caterpillars of *Eriogaster lanestris*. Naturwissenschaften **87**:193–196.

Ruf, C., and K. Fiedler. 2002. Tent-based thermoregulation in social caterpillars of *Eriogaster lanestris* (Lepidoptera: Lasiocampidae): behavioural mechanisms and physical features of the tent. Journal of Thermal Biology **27**:493–501.

Scheirs, J., L. De Bruyn, and R. Verhagen. 2001. Nutritional benefits of the leaf-mining behavior of two grass miners: a test of the selective feeding hypothesis. Ecological Entomology **26**:509–516.

Seymour, R. S., C. R. White, and M. Gibernau. 2003. Heat rewarding for insect pollinators. Nature **426**:243–244.

Spotila, J. R., O. H. Soule, and D. M. Gates. 1972. The biophysical ecology of the alligator: heat energy budgets and climate spaces. Ecology **53**:1094–1102.

Turner, J. S. 2000. The extended organism: the physiology of animal-built structures. Harvard University Press, Cambridge, Massachusetts, USA.

Van Dyck, H., and E. Matthysen. 1998. Thermoregulatory differences between phenotypes in the speckled wood butterfly: hot perchers and cold patrollers? Oecologia **114**: 326–334.

van Loon, J. J. A., J. Casas, and S. Pincebourde. 2005. Nutritional ecology of insect–plant interactions: persistent handicaps and the need for innovative approaches. Oikos **108**:194–201.

von Caemmerer, S., and G. D. Farquhar. 1981. Some relationships between the biochemistry of photosynthesis and the gas exchange of leaves. Planta **153**:376–387.

Ziegler, H. 1987. The evolution of stomata. *In* E. Zieger, G. D. Farquhar, and I. Cowan, editors. Stomatal function. Stanford University Press, Stanford, California, USA.